THE ASTROPHYSICAL JOURNAL, 342:1187–1206, 1989 July 15

OSCILLATIONS OF SOLAR MODELS WITH INTERNAL ELEMENT DIFFUSION

ARTHUR N. COX, JOYCE A. GUZIK[1], AND RUSSELL B. KIDMAN
Los Alamos National Laboratory
Received 1987 October 30; accepted 1988 December 22

ABSTRACT

Two precision solar models have been constructed with the Iben evolution program, one with no diffusion of the internal atomic nuclei and another that includes the effects of gravitational settling, thermal diffusion, and concentration gradient diffusion on the element abundances. Our pressure and energy equation of state and opacity have been specially fitted to the latest theoretical data. Then the opacity at the bottom of the convection zone was increased 15%–20% (within its theoretical uncertainty) to allow a better agreement with the observed solar p-mode frequencies. Our theoretical p-mode frequencies are now only a few microhertz less than those observed. The solar mass, radius, and luminosity, at an age of $4.6 \pm 0.06 \times 10^9$ yr, were matched for both evolution runs so that the theoretical uncertainty of the predicted oscillation frequencies was less than 1 μHz. Parameters adjusted to match the observed $M_\odot$, $R_\odot$, and $L_\odot$ were the initial helium abundance and the ratio of the mixing length to the pressure scale height in the normal convection theory. The original helium mass fractions of the mixtures were 0.291 and 0.289 for the no-diffusion and diffusion models, respectively. The diffusion model evolved to a surface $Y = 0.256$ at the solar age, and the original Z value of 0.0200 decreased to 0.0179 by diffusive settling. Our equation of state gives pressures that average maybe 1% too large throughout the Sun, and therefore more helium, with its lower pressure per gram than hydrogen, is needed to compensate for this small error. We estimate that the true helium mass fraction may be up to 0.01 smaller than what we use. The bottom of our convection zone is hotter than for most previous models because we have tried to match the measured p-mode frequencies, but it is probably not hot enough to deplete the surface lithium abundance to the observed value unless there is a small amount of overshooting below the bottom of the convection zone by about half a pressure scale height. It is possible that theoretical uncertainties in the pressure from the equation of state will always prevent matching the helium abundance (Y) and the p-mode frequencies to better than 0.005 and a few microhertz, respectively. A discussion is given of the agreement of asymptotic theory $l = 0$ and $l = 2$ p-mode frequency separations and those calculated directly with nonadiabatic theory. Calculation of g-mode solutions shows that they do not have equal period spacings until moderate radial order. Nonadiabatic solutions for these g-modes enable us to predict their relative surface visibility. For $l = 1$–5, the lowest order modes seem to be more detectable, assuming that they will all have the same kinetic energy. The high helium needed with our pressure equation of state results in high central temperatures that give over 9 SNU from the ^{8}B and 1.5 SNU from the ^{7}Be reactions, but a lower helium abundance, that we estimate, would reduce this ^{8}B neutrino flux maybe 2 SNU.

Subject headings: diffusion — Sun: interior — Sun: oscillations

I. BACKGROUND

Global oscillations of the Sun have received considerable observational interest in the last 20 years. Frequencies for low-degree p-modes (Pallé *et al.* 1986) and both low- and high-degree p-modes (Duvall *et al.* 1988; Libbrecht and Kaufman 1988) are now typically measured to an accuracy of better than about 1 μHz in 3000. Further observations are now being made to see if these frequencies vary with the solar activity cycle as proposed by van der Raay (1984), Woodard and Noyes (1985), Henning and Scherrer (1986), and Fossat *et al.* (1987). Also the splitting of these mode frequencies for a given order (n) and degree (l) is being actively studied to give the internal rotation structure of the Sun (see, e.g., Brown 1987*a*). However, theoretical models of the Sun are not able to predict global oscillation frequencies with anywhere near the observational accuracy. Some successful work on this problem is reported in this paper.

Recent pulsation studies of theoretical models of the Sun, based on evolution from a chemically homogeneous main-sequence state, have been published by Christensen-Dalsgaard (1982), Shibahashi, Noels, and Gabriel (1983), Ulrich and Rhodes (1983), Noels, Scuflaire, and Gabriel (1984), Scuflaire, Gabriel, and Noels (1984), Kosovichev and Severny (1984), Gabriel (1984), Lebreton and Maeder (1986), Kidman and Cox (1987), Lebreton and Maeder (1987), Bahcall and Ulrich (1988), and Guenther and Sarajedini (1988). Other pulsation results, based on models other than their own, were given by Provost (1984); Cox (1984), Berthomieu, Provost, and Schatzman (1984), Cox and Kidman (1984), Schatzman (1985), Kidman and Cox (1984), and Cox, Kidman, and Newman (1985). Two very provocative papers by Faulkner, Gough, and Vahia (1986) and Däppen, Gilliland, and Christensen-Dalsgaard (1986) are useful for their predicted oscillation frequencies since they relate to unconventional solar models with low central temperatures and neutrino fluxes.

In this work we report the results of the evolution of a solar model using our best available material property data and including the effects of diffusive processes that lead to a partial sorting of the elements with depth. Our two models are without and with the effects of diffusion. Our diffusion processes of gravitational settling. composition gradient diffusion, and thermal diffusion are adapted from and added to the

[1] Also Astronomy Program, Department of Physics, Iowa State University.

method described by Iben and MacDonald (1985). While the surface abundances of helium and the heavier elements are decreased at the solar age relative to the case of no diffusion, the pulsation frequencies are not much changed. Important results of our work are that a high original helium content ($Y = 0.29$) is required to match the observed global oscillation data, and the total neutrino flux detectable by the chlorine detector accordingly is increased to over 10 SNU.

II. MATERIAL PROPERTIES

The accuracy of the calculated frequencies from solar models depends strongly on the accuracy of the material properties used to develop the model. These properties are in three categories: equation of state, opacity, and nuclear energy production. The energy production seems to have little uncertainty, even though we have used only the older Fowler, Caughlin, and Zimmerman (1975) reaction rates for this study.

Uncertainties in the equation of state are important mainly for the *p*-modes that strongly sample the solar convection zone. This convection zone structure depends both on the pressure and energy parts of the equation of state, because the amount of convection depends not only on the pressure the gas can produce by its nuclei and free electrons but also on how superadiabatic the temperature gradient is. Within the convection zone of the model, the adiabatic value of the gradient $(dT/T)/(dP/P)$ is equal to the $\Gamma_3 - 1$ to Γ_1 ratio [also equal to $(\Gamma_2 - 1)/\Gamma_2$]. This gradient is less than the gradient needed to establish hydrostatic equilibrium and the required photon luminosity flow. The exact difference between the gradients and the magnitude of the adiabatic gradient itself are important.

The composition used for this material property comparison work is given in Table 1 for our 12 elements. It is that used by Cox and Tabor (1976) and is representative of the solar surface and the homogeneous composition convection zone. Both number and mass fractions are listed. Note, however, that for the evolution and element diffusion calculations, only eight completely ionized isotopes were considered.

Convection zone conditions for the diffusion model are given in Table 2, which gives the temperature, density, $\Gamma_3 - 1$, Γ_1, and the gas pressure constant $b' = PV/T$ from detailed calculations. The calculated data come from (Mihalas, Däppen, and Hummer 1988), who have specially computed a precision equation of state for the solar mixture. Their results agree very well with the much older equation of state data from EXOP, the (expanded) opacity program that was for years the basic program for all the Los Alamos opacities.

TABLE 1

COMPOSITION FOR THE SOLAR MIXTURE ($Z = 0.02$)

Element	Number Fraction	Mass Fraction
H	9.07156E−01	7.00000E−01
He	9.13793E−02	2.80000E−01
C	2.84436E−04	2.61540E−03
N	8.01664E−05	8.59600E−04
O	6.36796E−04	7.79960E−03
Ne	3.58814E−04	5.54400E−03
Na	1.42048E−06	2.49999E−05
Mg	1.79456E−05	3.34000E−04
Al	1.19097E−06	2.46000E−05
Si	2.27711E−05	4.89601E−04
Ar	2.38377E−05	7.29000E−04
Fe	3.69376E−05	1.57920E−03

In EXOP ionization of all the individual elements and their ions is calculated by procedures given by Cox (1965). The gas pressure includes variable ionization to account for the available free electrons, the appropriate small amount of pressure increase from electron degeneracy, and a slight decrease from the Coulomb effects. Radiation pressure is also included, even though it contributes less than 0.1% to the total. We do not discuss in much detail the differences between EXOP and the Mihalas data here, because they are quite small, as one would expect from methods that are very similar. Nevertheless, looking at the uncertainties in computing the internal partition functions in the ionization calculations, it is probably never going to be possible to calculate the gammas and the pressure more accurately than about 1%, especially in the convection zone.

Stellar evolution studies require knowing the equation of state and opacity for compositions that vary both in space throughout the model and in time as the model evolves. We, like many others, have therefore been forced to use a set of procedures for these material properties that have been calibrated to match existing tables for their compositions as well as possible.

We have adopted and calibrated the Iben (1963) procedure (based on a method discussed in detail by Demarque 1960 and

TABLE 2

CONVECTION ZONE EQUATION OF STATE

$T(10^6$ K)	ρ(g/cm^{-3})	$\Gamma_3 - 1$	Iben	Γ_1	Iben	$b'(10^8)$	Iben (10^8)
1.4818	9.539E−2	0.659	0.662	1.664	1.667	1.328	1.322
1.0178	5.420E−2	0.659	0.661	1.664	1.668	1.325	1.318
0.4974	1.843E−2	0.657	0.657	1.668	1.668	1.330	1.305
0.3026	8.668E−3	0.650	0.647	1.667	1.664	1.300	1.290
0.2024	4.618E−3	0.626	0.617	1.651	1.644	1.280	1.271
0.1012	1.327E−3	0.520	0.528	1.555	1.564	1.233	1.214
0.0898	1.056E−3	0.526	0.540	1.560	1.576	1.224	1.203
0.0794	8.429E−4	0.541	0.551	1.577	1.590	1.215	1.192
0.0702	6.738E−4	0.552	0.547	1.592	1.591	1.206	1.180
0.0576	4.627E−4	0.517	0.498	1.573	1.550	1.178	1.156
0.0499	3.396E−4	0.474	0.440	1.537	1.495	1.167	1.134
0.04009	1.932E−4	0.365	0.351	1.437	1.405	1.119	1.094
0.03011	7.612E−5	0.282	0.272	1.357	1.326	1.055	1.030
0.02007	1.282E−5	0.181	0.182	1.251	1.239	0.922	0.911
0.01002	3.591E−7	0.175	0.180	1.217	1.222	0.666	0.668
0.00598	2.591E−7	0.631	0.633	1.634	1.636	0.638	0.641

Vardya 1964) that computes the ionization of only the hydrogen electron, the two helium electrons, and a single electron from a representative heavy element with an ionization potential of 7.5 eV. The justification for this simple procedure is that the heavy elements of a solar mixture contribute less than 1% of the free particles that cause pressure. The Iben procedure makes the further approximation that the ratio of the internal partition functions needed for the ionization equilibrium calculation is equal to the ratio of the ground-state statistical weights.

The results of the calibration are shown in Table 2 for the composition given in Table 1. Given beside the two gamma and b' values are the values obtained from our modified Iben procedure. The agreement between the gammas can be seen to be usually better than 0.01, with somewhat larger differences at temperatures lower than 90,000 K in the hydrogen and helium ionization zones that are only 1.3% of the radius and 4.5×10^{-6} of the mass into the Sun. The maximum differences for the gammas are at 50,000 K (over 0.03 for $\Gamma_3 - 1$ and over 0.04 for Γ_1), apparently because the Iben procedure does not calculate the second helium ionization so elaborately. Only a small part of these differences comes from the interpolation necessary in the Mihalas data at the second ionization temperature of He, where values change rapidly.

Incidentally, the EXOP code results are in better agreement with the modifed Iben procedure, with maximum differences of $\Gamma_3 - 1$ being 0.02 high at 40,000 K and Γ_1 being 0.02 low at 20,000 K.

At 50,000 K, the b' from the Iben procedure, modified by us to include Coulomb pressure-reducing effects, is 3% too low, but the pressure is generally accurate to better than 1%. Shibahashi, Noels, and Gabriel (1983) and Stix and Knoelker (1986) have discussed the important effects on models and p-mode oscillation frequencies when the Coulomb effects are included.

It is important to realize that the oscillation frequency squared in simple adiabatic radial oscillations involves a term with the factor $3\Gamma_1 - 4$ and another term with Γ_1 as a factor. Another way of thinking about the role of Γ_1 is that the sound velocity of the acoustic p-modes varies as its square root, and the sonic transit time through the star determines its oscillation period. Thus, with uncertainties of almost 1% in Γ_1, averaged over the ionization zone region where, say, a p-mode feels the structure of the star, the frequency can be uncertain by some fraction of 1%. Thus, unless the Γ_1 can be made considerably more accurate than what we currently have, agreement with the observed p-mode frequencies to better than a few μHz, that is, to 0.1%, does not seem possible with present solar composition equations of state. However, presumably our calibration of the Iben procedure for the ionization could be improved.

In the outer layers, where our evolution program gamma values compare less well with those calculated more accurately, the modes with l greater than several hundred have great weight for their period determination. These are layers where the temperature is less than 60,000 K. Nevertheless, theoretical frequencies seem to agree reasonably well with observations, as we see later. Only for $l = 200$ or more, where only the hydrogen ionization zone is sampled, does there seem to be a significant additional effect of the gamma errors on the comparison between theoretical and observed p-mode frequencies.

Table 3 gives the opacity and pressure ($b' = PV/T$) for pairs or triplets of temperatures for densities that closely track our solar model. The effect of varying hydrogen content toward the solar center is accounted for by switching to different composition tables at the high temperatures. The low temperature table, called Ross-Aller 1, was calculated by the molecular opacity program (MOOP), which is the EXOP program (for a description see Cox 1965) modified in several aspects, including the addition of molecular absorptions. The higher temperature opacities come from mixtures calculated from the Astrophysical Opacity Library (Huebner, Merts, and Magee 1977). Comparisons with the Iben procedure are again given, and one can see that this method gives systematically larger pressures at temperatures above 10^5 K, in the layers near the bottom of the convection zone in the Sun. Such an effect was predicted by Graboske (1972). It is probably caused by the lower weight given to the last ionization stage relative to the completely ionized atom by using only approximate internal partition functions. At temperatures around 5×10^4 K, Coulomb effects (after Clayton 1968, p. 144) reduce the pressure by as much as 6%.

The small amount of extra pressure in the Iben procedure is compensated for by our being forced to reduce hydrogen (by maybe 0.01 in X) throughout the solar model in order to obtain the observed luminosity and radius of the Sun at its age of 4.6×10^9 yr. One can see that an error of $\delta P/P$ relates to a δY change by the following reasonably accurate formula based on complete ionization, appropriate for all but about the outer 1% of the solar mass:

$$\delta P/P = -5\,\delta Y/4(2X + 3Y/4 + Z/2)\,,$$

where X, Y, and Z are the mass fractions of the solar composition for, respectively, hydrogen, helium, and the assumed fixed mass fraction for all the heavier elements. For this equation we assume that all the pressure is from the gas with no corrections for its very slight electron degeneracy, Coulomb effects, or for the very small amount of radiation pressure. Evaluating this expression for the composition $X = 0.70$, $Y = 0.28$, and $Z = 0.02$, we get $\delta Y = -1.3\,\delta P/P$. This is only an approximate evaluation for the required helium abundance change due to an equation of state pressure error, because many other variables enter into the proper solar structure and evolution calculation.

It is possible to see that the extra helium required to keep the internal pressure down has little effect on the opacity. From Table 3 we see that a change from $Y = 0.28$ to 0.38 gives a decrease of 30% in the opacity at a density of 10 g cm^{-3} and a temperature of 5×10^6 K. Similar helium content changes at higher temperatures and densities give even smaller opacity changes. Thus a change in Y by 0.01 probably produces only 3% or less opacity change for the bulk of the solar mass.

Complete ionization occurs at a temperature less than 2×10^6 K. However, we have switched from the ionization calculation procedure to complete ionization in the Iben program at 4.5×10^6 K to be sure of a reasonably smooth transition, especially for the Brunt-Väisälä frequency. At higher temperatures, where a slight amount of electron degeneracy occurs, the Eggleton *et al.* (1973) method is used as part of the Iben procedure.

In place of the Iben procedure at low temperature, we use a fit to the opacity developed by Stellingwerf (1975*a*, *b*) and modified here for temperatures less than 10^6 K. To allow for molecular absorptions (mostly water vapor), the Stellingwerf opacities in the calculations and in Table 3 are multiplied by a factor of 3. Above 9000 K the very high opacities produce a

large temperature gradient that is entirely fixed by convection, so the exact opacity values are not important.

The Iben (1975) procedure for the opacity that we use for layers deeper than the convection zone has been adjusted both to fit the latest Opacity Library values, and also to fit the p-mode frequencies better. In the expression for the Z effect, called A_z, a factor of 1.30 has been added. Also the κ_e electron scattering term has been doubled to better match the more modern central opacity. These modified opacities are in Table 3. Detailed comparisons show that between 2 and 7 × 10^6 K the Iben procedure opacities are 15%–20% larger than those given by the latest Opacity Library values, and this increase has been made deliberately to improve agreement with the observed p-mode frequencies. This opacity increase was suggested to us by Korzennik and Ulrich (1989), who have made detailed studies of how improvement between observed and theoretical oscillation frequencies can be attained. An opacity increase was also suggested earlier by Christensen-Dalsgaard *et al.* (1985). According to A. L. Merts (1988, private communication) such an increase is within the theoretical uncertainty of the opacity at these temperatures and densities. At temperatures above 10^7 K the agreement with the Opacity Library is within 5%, with the central opacity from the Iben procedure being too small. The main effects, as will be seen later, are that the convection zone is deeper than any previous model based on evolution, and the central temperature is just

TABLE 3

SOLAR OPACITY AND PRESSURE EQUATION OF STATE

A. ROSS-ALLER 1: $X = 0.700$, $Y = 0.280$, $Z = 0.020$

ρ(g cm^{-3})	T(K)	κ(cm^2 g^{-1})	Stellingwerf	b'(ergs g^{-1} K^{-1})	Iben
1.00E−08.....	4.64E+03	2.012E−02	2.576E−02	6.365E+07	6.406E+07
	5.80E+03	6.706E−02	1.390E−01	6.369E+07	6.410E+07
3.00E−08.....	4.64E+03	5.652E−02	6.225E−02	6.362E+07	6.404E+07
	5.80E+03	1.590E−01	2.277E−01	6.368E+07	6.408E+07
	6.96E+03	1.232E+00	1.883E+00	6.389E+07	6.430E+07
1.00E−07.....	4.64E+03	1.628E−01	1.490E−01	6.356E+07	6.398E+07
	5.80E+03	3.944E−01	4.124E−01	6.366E+07	6.407E+07
	6.96E+03	2.134E+00	2.914E+00	6.378E+07	6.419E+07
3.00E−07.....	4.64E+03	3.374E−01	2.950E−01	6.338E+07	6.380E+07
	5.80E+03	8.436E−01	7.546E−01	6.364E+07	6.404E+07
	6.96E+03	3.628E+00	4.489E+00	6.373E+07	6.413E+07
1.00E−06.....	6.96E+03	6.888E+00	7.460E+00	6.368E+07	6.408E+07
	9.28E+03	7.244E+01	1.479E+02	6.451E+07	6.490E+07
3.00E−06.....	6.96E+03	1.237E+01	1.224E+01	6.361E+07	6.402E+07
	9.28E+03	1.067E+02	2.022E+02	6.414E+07	6.454E+07

B. COX-DAVIS 6: $X = 0.700$, $Y = 0.280$, $Z = 0.020$

ρ(g cm^{-3})	T(K)	κ(cm^2 g^{-1})	Stellingwerf/Iben	b'(ergs g^{-1} K^{-1})	Iben
1.00E−06.....	1.20E+04	7.621E+02	1.400E+03	7.018E+07	7.058E+07
	1.30E+04	1.282E+03	2.578E+03	7.476E+07	7.498E+07
3.00E−06.....	1.45E+04	...	...	7.643E+07	7.648E+07
	1.60E+04	...	...	8.456E+07	8.419E+07
1.00E−05.....	1.80E+04	...	...	8.495E+07	8.428E+07
	2.00E+04	...	...	9.357E+07	9.322E+07
5.00E−05.....	2.25E+04	...	...	8.966E+07	8.712E+07
	2.50E+04	...	...	9.698E+07	9.475E+07
	2.80E+04	...	...	1.041E+08	1.026E+08
1.00E−04.....	2.80E+04	...	...	9.883E+07	9.543E+07
	3.20E+04	...	...	1.062E+08	1.039E+08
5.00E−04.....	5.20E+04	...	...	1.134E+08	1.116E+08
	5.60E+04	...	...	1.150E+08	1.141E+08
	6.00E+04	...	...	1.163E+08	1.167E+08
1.00E−03.....	7.00E+04	...	...	1.157E+08	1.152E+08
	8.00E+04	...	...	1.179E+08	1.183E+08
	9.00E+04	...	...	1.197E+08	1.206E+08
2.00E−03.....	1.00E+05	...	...	1.187E+08	1.188E+08
	1.30E+05	...	...	1.230E+08	1.241E+08
5.00E−03.....	1.60E+05	...	...	1.224E+08	1.230E+08
	2.00E+05	...	...	1.250E+08	1.266E+08
1.00E−02.....	2.00E+05	...	...	1.220E+08	1.230E+08
	3.00E+05	...	...	1.262E+08	1.310E+08
	5.00E+05	...	...	1.293E+08	1.330E+08
3.00E−02.....	5.00E+05	...	...	1.263E+08	1.318E+08
	7.00E+05	...	...	1.286E+08	1.329E+08
1.00E−01.....	1.30E+06	5.108E+01	8.520E+01	1.300E+08	1.335E+08
	1.60E+06	3.235E+01	5.209E+01	1.315E+08	1.338E+08
1.00E+00.....	3.00E+06	1.951E+01	1.921E+01	1.310E+08	1.338E+08
	5.00E+06	2.891E+00	4.163E+00	1.322E+08	1.343E+08
1.00E+01.....	5.00E+06	7.702E+00	7.797E+00	1.321E+08	1.342E+08
	7.00E+06	2.816E+00	3.210E+00	1.324E+08	1.344E+08

TABLE 3—*Continued*

C. KING-III*a*: $X = 0.600$, $Y = 0.380$, $Z = 0.020$

ρ(g cm^{-3})	T(K)	κ(cm^2 g^{-1})	Iben	b'(ergs g^{-1} K^{-1})	Iben
1.00E+01.....	5.00E+06	5.423E+00	7.645E+00	1.235E+08	1.237E+08
	1.00E+07	1.038E+00	1.396E+00	1.235E+08	1.242E+08
1.00E+02.....	1.00E+07	2.443E+00	2.687E+00	1.235E+08	1.262E+08
	2.00E+07	7.486E−01	8.939E−01	1.235E+08	1.250E+08

D. COX-HODSON 7: $X = 0.500$, $Y = 0.480$, $Z = 0.020$

ρ(g cm^{-3})	T(K)	κ(cm^2 g^{-1})	Iben	b'(ergs g^{-1} K^{-1})	Iben
1.00E+01.....	5.00E+06	7.301E+00	7.508E+00	1.117E+08	1.133E+08
	1.00E+07	1.104E+00	1.319E+00	1.121E+08	1.138E+08
1.00E+02.....	1.00E+07	3.035E+00	2.572E+00	1.138E+08	1.154E+08
	2.00E+07	7.896E−01	8.415E−01	1.130E+08	1.145E+08

E. COX-HODSON 6: $X = 0.400$, $Y = 0.580$, $Z = 0.020$

ρ(g cm^{-3})	T(K)	κ(cm^2 g^{-1})	Iben	b'(ergs g^{-1} K^{-1})	Iben
1.00E+01.....	5.00E+06	7.084E+00	7.388E+00	1.015E+08	1.029E+08
	1.00E+07	1.052E+00	1.246E+00	1.018E+08	1.034E+08
1.00E+02.....	1.00E+07	2.921E+00	2.462E+00	1.033E+08	1.047E+08
	2.00E+07	7.510E−01	7.900E−01	1.027E+08	1.040E+08

F. COX-HODSON 5: $X = 0.300$, $Y = 0.680$, $Z = 0.020$

ρ(g cm^{-3})	T(K)	κ(cm^2 g^{-1})	Iben	b'(ergs g^{-1} K^{-1})	Iben
1.00E+01.....	5.00E+06	6.855E+00	7.283E+00	9.134E+07	9.246E+07
	1.00E+07	9.986E−01	1.175E+00	9.162E+07	9.300E+08
1.00E+02.....	1.00E+07	2.800E+00	2.357E+00	9.286E+07	9.404E+07
	2.00E+07	7.118E−01	7.394E−01	9.245E+07	9.356E+07

slightly too small. These higher opacities also require higher helium, just as the pressure systematic errors do, because the higher opacity must be compensated for by adding more lower intrinsic opacity helium.

III. DIFFUSION PROCEDURES

The diffusion of elements in the Sun has been considered previously by Noerdlinger (1977), Gabriel, Noels, and Scuflaire (1983), Demarque and Guenther (1986), and Wambsganss (1988). Here we include more details. The effects of both pressure and thermal diffusion are incorporated into our second solar model according to the method of Burgers (1969, pp. 92–97). The diffusion equations and heat flow equations, plus two equations imposing the conditions of no net mass or current flow are solved simultaneously:

$$\nabla p_i - \frac{\rho_i}{\rho}\nabla p - n_i q_i E = \sum_j K_{ij}(w_j - w_i) + \sum_j K_{ij} z_{ij} \frac{m_j r_i - m_i r_j}{m_i + m_j},$$

$$\frac{5}{2} n_i k \nabla T = -\frac{5}{2}\sum_{j\neq i} K_{ij} z_{ij} \frac{m_j}{m_i + m_j}(w_j - w_i) - \frac{2}{5} K_{ii} z''_{ij} r_i - \sum_{j\neq i} \frac{K_{ij}}{(m_i + m_j)^2}(3m_i^2 + m_j^2 z'_{ij} + 0.8 m_i m_j z''_{ij}) r_i + \sum_{j\neq i} \frac{K_{ij} m_i m_j}{(m_i + m_j)^2}(3 + z'_{ij} - 0.8 z''_{ij}) r_j,$$

$$\sum A_i n_i w_i = 0, \qquad \sum Z_i n_i w_i = 0.$$

Here i is any one of the eight diffusing elements, and j stands for all the others in interactions and sums, with charge q_j, mass m_j, atomic weight A_j, and atomic number Z_j.

The unknowns are the diffusion velocities (w_i) and the magnitudes of the residual heat flow vectors (r_i) of each ionic species plus the electron, and the electric field (E). The pressure gradient terms on the left-hand side of the diffusion equation can be rewritten into three terms by substituting the condition for hydrostatic equilibrium, $\nabla p = -\rho g$, and the ideal gas equations for the partial pressures of each particle species, $p_i = n_i kT$, and then dividing by n_i:

$$-A_i m_H g - kT \frac{d\ln T}{dr} - kT \frac{d\ln n_i}{dr}.$$

The first two terms, containing the gravitational acceleration and the temperature gradient, are considered together as the forcing terms for "gravitational" diffusion. The last term, containing the composition gradient, drives chemical diffusion.

We adapted the subroutine and procedure described by Iben and MacDonald (1985) to include thermal diffusion by adding the heat flow equations. The diffusion of 10 ionic species is followed: H, ^{3}He, ^{4}He, ^{12}C, ^{14}N, ^{16}O, ^{18}O, ^{22}Ne, ^{21}Ne, and ^{25}Mg (in our models, ^{21}Ne and ^{25}Mg have zero abundances). Thus we solve, at each time step, 23 equations—a diffusion equation for each of the 10 ions, a heat flow equation for each ionic species plus the electron, the equation for no net mass flow, and the equation for no net current flow—for 23 unknowns, 11 w_i's, 11 r_i's, and the electric field E. Iben and MacDonald calculate the resistance coefficients (K_{ij}) using an analytical fit to the binary diffusion coefficients of Fontaine and Michaud (1979) that are derived using screened Coulomb potentials:

$$K_{ij} = 1.6249 \ln(1 + 0.18769 x_{ij}^{1.2}) \frac{2^{3/2}}{3} \pi^{1/2} \mu_{ij}^{1/2} \frac{e^4 Z_i^2 Z_j^2}{(kT)^{3/2}} n_i n_j,$$

where

$$\mu_{ij} = A_i A_j m_H/(A_i + A_j)$$

is the reduced mass of the interacting particles, and

$$x_{ij}^2 = \frac{16k^2T^2}{Z_i^2 Z_j^2 e^4}\lambda^2 ,$$

where λ is the larger of the Debye length

$$\lambda_D = \left(\frac{kT}{4\pi e^2 \sum_i n_i Z_i^2}\right)^{1/2}$$

and the mean ionic separation is given by

$$a_0 = \left(\frac{3}{4\pi \sum_{\text{ions}} n_i}\right)^{1/3} .$$

These coefficients are meant to apply to the wide region of the temperature-density plane spanned by conditions in white dwarfs, specifically, $-2 \lesssim \phi \lesssim 2$, where $\phi = \ln[\ln(1 + x_{ij}^2)]$, but the analytical fit by Iben and MacDonald is in excellent agreement with the tabulated values of Fontaine and Michaud (1979), as well as with the fit of Muchmore (1984) for much smaller range of temperatures and densities in the solar interior, i.e., $\phi \cong 2.2$. Nevertheless, Iben and MacDonald caution that the errors in the resistance coefficients may be greater than 10%. The heat flow resistance coefficients z, z', and z'' are, respectively, 0.6, 1.3, and 2.0 (from Muchmore 1984).

The method of Burgers (1969) assumes (1) negligible radiative forces, (2) complete ionization, (3) Maxwellian velocity distributions and the same kinetic temperature for all ions and electrons, (4) diffusion velocities which are much smaller than mean thermal velocities, (5) no magnetic fields, (6) collisions dominated by "classical" interactions between two point particles, and (7) plasma which can be considered a dilute gas, i.e., the ideal gas equation of state applies. The validity of these assumptions is discussed by Iben and MacDonald (1985), Fontaine and Michaud (1979), and Paquette *et al.* (1986). In Burgers's (1969, pp. 151–153) formulation, all species are treated symmetrically, so the equations themselves are valid when any one isotope is not a trace constituent relative to hydrogen, as is the case for ^{4}He in main-sequence stars. However, the diffusion coefficients of Fontaine and Michaud (1979) are calculated assuming ^{4}He is a trace constituent. Fontaine and Michaud argue that the errors introduced are insignificant compared to the inherent errors which are due to other assumptions. Roussel-Dupré (1982 finds from his study of thermal diffusion in ternary gas mixtures (H, He, and electrons) that the corrections of Burgers's thermal diffusion coefficient for ionized ^{4}He/H abundances characteristic of the Sun are negligible.

Many authors (e.g., Roussel-Dupré 1982; Muchmore 1984; Paquette *et al.* 1986; Monchick and Mason 1985) recognize the problem of the "small plasma parameter" inherent in the environments of the interiors of both white dwarfs and main-sequence stars. When the number of particles in a Debye sphere around an ion is not $\gg 1$, assumptions (6) and (7) above are inappropriate. Ions are no longer effectively screened from their surroundings, and multiple particle collisions and collective effects become important. The "classical" approach to calculating transport properties of ions using Boltzmann's equation becomes invalid. In the Sun, the number of particles per Debye sphere is only about 1.4 at the base of the convection zone, and 2.2 at the core, so the "dilute gas" approximation fails. Monchick and Mason (1985) report that the inclusion of quantal effects (introduced because electrons are not classical point particles) and dynamical shielding will reduce the diffusion coefficient by 40%–50% in conditions appropriate to the solar convection zone base, with most of this reduction caused by dynamical shielding. Including collective effects will thus substantially reduce the amount of diffusion, so the amount of diffusion calculated in our model should only be considered an upper limit to that actually occurring in the Sun.

Since the composition of part of the Sun's envelope is rehomogenized by convection, diffusion is important only below the convection zone base, at temperatures greater than about 2.1×10^6 K, and densities greater than 0.1 g cm^{-3}, where diffusing elements are almost completely ionized. We find typical total ion diffusion velocities of a few times 10^{-10} cm s^{-1} at the solar center, and nearly 10^{-8} cm s^{-1} at the base of the convection zone. Including the effects of thermal diffusion more than doubles the diffusion velocities at the base of the convection zone. Thermal diffusion acts in the same direction as gravitational settling, i.e., driving the ions up the temperature gradient toward the solar center, for reasons explained by Roussel-Dupré (1981). Since the electrons have faster mean thermal velocities than the ions for a given temperature, they are first to move from hot to cold regions, down the temperature gradient. To maintain the condition of no net current flow, cold electrons must replace these, flowing up the temperature gradient. These cold electrons have a higher interaction cross section with ions than the hot electrons and thus transfer their momentum to the ions, causing them to flow up the temperature gradient. Chemical diffusion is a relatively minor effect, adding at most 10%–20% to the diffusion velocity of a given species in regions of strong composition gradients, e.g., for ^{4}He in the core at later stages of evolution, in this case opposing the tendency of thermal and gravitational diffusion to concentrate ^{4}He toward the center.

One should note that our diffusion effects assume that there is no turbulent diffusion in the Sun that can cause mixing such as most recently discussed by Lebreton and Maeder (1987). Actually turbulence is suppressed in composition gradient regions, and if the settling of helium and the Z elements is fast enough, no mixing can occur at all. Deep in the present Sun, the gradient $(dT/T)/(dP/P)$ is subadiabatic by at least 0.08. The place where the gradient is just barely subadiabatic is just below the convection zone, and occasionally suggestions have been made that some turbulent mixing could occur there. However, the convection zone is exactly where our diffusive settling is fastest and is likely to suppress all mixing.

There has been concern that early in the solar main-sequence life, some mixing of hydrogen into the central region and even possibly convection may have occurred as a result of pulsation instability caused by ^{3}He or even ^{12}C nuclear energy generation (ϵ) effects that can destabilize g-modes. These were discussed long ago by Dilke and Gough (1972). A problem with calculations of these possible instabilities is that the damping effects of the convection zone are never accurately considered (see Saio 1980). Our reasonably good match to observed solar oscillation frequencies indicates that these mixing events were at best very small. Our evolution calculation never produces any core convection.

IV. MODELS

Evolution calculations were made using the Iben evolution program (originally described in 1965) with modifications discussed above for the equation of state, for the opacity, and for the element diffusion. Details of the results of the two evolution

TABLE 4

SOLAR EVOLUTION RESULTS

Parameter	Without Diffusion	With Diffusion
Initial Y	0.291	0.289
Initial Z	0.020	0.020
Mixing length ratio	1.894	1.951
Zones	454	402
Time steps	328	320
Age (10^9 yr)	4.66	4.54
Luminosity ($L_\odot$)	1.00013	1.00049
Radius ($R_\odot$)	1.00000	1.00000
$T_{\rm eff}$(K)	5770.7	5771.2

calculations are in Table 4. Standard mixing length theory (Cox and Giuli 1968, p. 209) is used, with an adjustment of the mixing length to match the solar radius. The effects of turbulent pressure are ignored. Note that the evolution runs were done with over 300 time steps, in contrast to the more typical case of 10 steps as most recently used by Guenther and Sarajedini (1988). The required mixing lengths in units of the pressure scale height are just slightly higher than conventional. The radius for the models at the solar age matches the solar radius to allow accuracy to better than 1 μHz in the p-mode frequencies.

We have assumed that the solar mass is 1.989×10^{33} g, the solar radius is 6.9599×10^{10} cm, and the solar luminosity is 3.826×10^{33} ergs s^{-1}. This luminosity was suggested by Christensen-Dalsgaard in a private communication, but it seems small, and a check case at 3.862×10^{33} ergs s^{-1} was made to bracket the true solar luminosity. With all other parameters held fixed, except the required small increase in Y (by 0.001) and the mixing length (by 0.7%) to keep the radius fixed, the p-mode frequencies are only slightly changed, as we see later.

Results for the present Sun are in Tables 5 and 6. The small effect of heavy-element settling can be seen at the central Y and Z values. The higher central helium than conventional gives a higher central temperature and a higher neutrino flux at Earth. The largest effect on composition is seen in the great reduction of the surface Y and Z. For the neutrino flux in the chlorine detector we have used the latest cross section of 1.06×10^{-42} cm^2 as reported by Bahcall and Holstein (1986). Figure 1 plots the hydrogen mass fraction of the composition versus the internal mass for the diffusion case. The main effect is the settling of helium and the floating of hydrogen just below the homogeneous composition convection zone, although the central Y is also increased slightly.

TABLE 5

SOLAR INTERIOR RESULTS

Parameter	Without Diffusion	With Diffusion
Central Y	0.6556	0.6580
Central Z	0.0206	0.0214
Central $T(10^6$ K)	15.68	15.73
Central density (g cm^{-3})	162.4	163.3
B^8 neutrinos (SNU)	9.2	9.7
Be^7 neutrinos (SNU)	1.5	1.6

TABLE 6

SOLAR ENVELOPE RESULTS

Parameter	Without Diffusion	With Diffusion
Surface Y	0.2912	0.2556
Surface Z	0.0200	0.0179
Convection zone $T(10^6$ K)	2.290	2.142
Convection zone $R(R_\odot)$	0.714	0.721
Convection zone $M(M_\odot)$	0.975	0.977

The composition structure is taken from the Iben evolution models and is put into another program to construct a model with mass zoning suitable for nonradial pulsation analyses. Because of small differences in the treatment of the Z part of the composition when calculating the opacity between the evolution program and the model builder program for the pulsation analysis, the helium fraction needed to be changed throughout the entire model by $+0.00016$ in the no-diffusion and -0.00032 in the diffusion models to account exactly for all the mass, radius, and luminosity.

Figure 2 gives the relation between zone number and the zone-centered radii. We use the zone number as the abscissa in many of our plots to enhance, as needed, the spatial resolution of quantities. The bottom of the convection zone is at zone 1234, and the photosphere is in zone 1613. One can see that there is good resolution at the surface (to define well the p-modes) and the center (where the g-modes at low l have large amplitudes). The spatial resolution everywhere in the model exterior to the central 0.4% of the radius is at least as good as that used by Christensen-Dalsgaard according to data kindly supplied by him. Investigations by Guenther and Sarajedini (1988) show that with this zoning, we should have less than 0.6 μHz error in the predicted p-mode frequencies.

We believe that 1700 zones are adequate to resolve the surface p-modes and the deep g-modes, because adiabatic oscillation frequencies determined from the eigensolution eigenvalues agree with integrals of weight functions, some of which are displayed later. Experience shows that if there is not enough spatial resolution, there is a significant difference between the two ways of determining the pulsation frequencies. The integral of the weight function is the application of the variational principle (Cox 1980, p. 234; Christensen-Dalsgaard, Gough, and Morgan 1979), and this eigenvalue is the more accurate one, given the spatial resolution of the model.

The masses for the 1700 zones are plotted in Figure 3. With this mass zoning, the central ball has a mass of 4.5×10^{27} g and a radius of 1.9×10^8 cm.

The outer boundary condition for the temperature is

$$T^4 = T_{\rm eff}^4(\tau + \tfrac{2}{3}) ,$$

where τ is the Rosseland mean optical depth of the center of the outermost mass shell. In our models, the τ at the center of the last mass shell is 10^{-4}. We find this is sufficiently small to produce negligible influence on the oscillation frequencies (Ulrich and Rhodes 1983). For the pressure boundary condition, we assume that there is no radiation pressure in the last shell, zero pressure outside, and that the inertial mass of the last mass shell is multiplied by 7.7 (a relic factor frequently used in Los Alamos pulsation calculations with no particular justification) to approximate the overlying chromosphere and corona mass.

Figure 4 displays the Γ_1 and $\Gamma_3 - 1$ versus zone number in the convection zone for the model with no diffusion effects. The gas has both gammas almost equal to 5/3 deeper than the convection zone. Figure 5 plots the opacity for zones below the surface convection zone. Figure 6 shows the logarithmic partial derivative of the opacity with respect to the temperature, a key quantity for the evaluation of the nonadiabatic

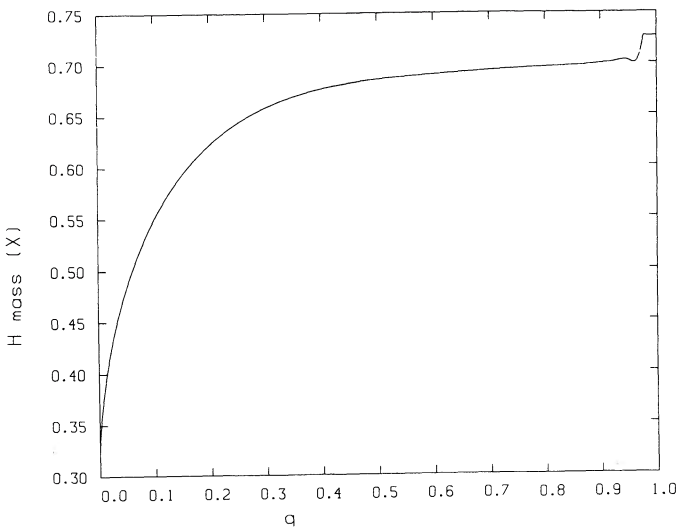

FIG. 1

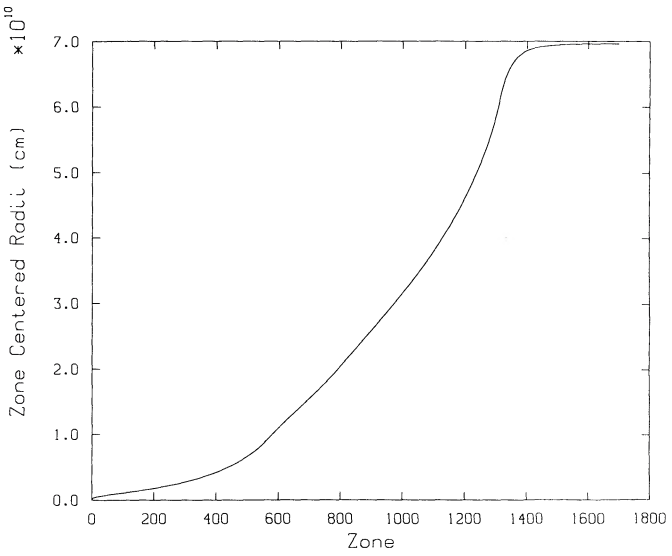

FIG. 2

FIG. 1.—The hydrogen mass fraction in the mixture is plotted vs. the internal mass fraction for the diffusion solar model. The spline fit to the composition structure obtained from the Iben evolution program gives slightly unphysical inward composition gradients at the surface (where X varies from 0.7265 down to 0.7260 and back to 0.7264) and at the bottom of the steep composition gradient below the homogeneous convection zone (where X varies from a minimum of 0.7000 up to 0.7027).

FIG. 2.—Zone-centered radii for the 1700 zones are plotted vs. the zone number. Good spatial resolution in this no-diffusion model exists both at the surface and at the center.

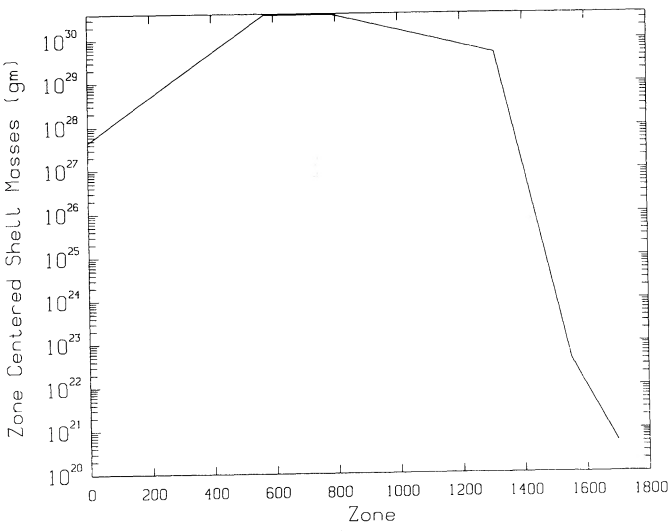

FIG. 3

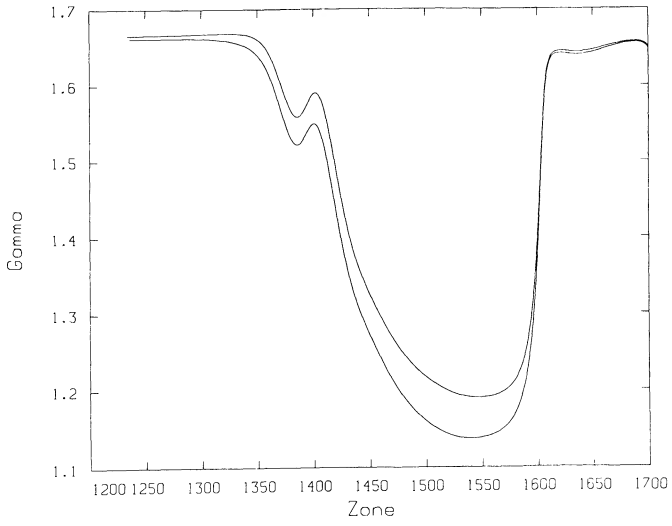

FIG. 4

FIG. 3.—Masses of all the 1700 shells are plotted vs. the zone number. The maximum shell mass is 0.002 of the solar mass. The thin surface zones are necessary for resolution of the high-degree p-modes. The fine zoning at the model center occurs in the central 15% of the radius.

FIG. 4.—Γ_1 (*upper curve*) and Γ_3 (*lower curve*) are plotted vs. zone number for the zones in the convection zone in the outer 30% of the radius in the no-diffusion model. The small dip at the surface is in the optically thin region, where there is a slight bit of hydrogen ionization. The main minima near zone 1550 are due to the ionization of hydrogen centered at 1.1×10^4 K, and the dip deepest into the model at 1.1×10^5 K is caused by the ionization associated with the last electron coming off helium. These effects are also seen in Table 2.

effects on the period and growth rate. Figure 7 shows the Brunt-Väisälä frequency, for the no-diffusion model, versus zone number.

V. p-MODE FREQUENCIES

The finely zoned model is introduced into our nonradial pulsation programs to calculate the adiabatic and nonadiabatic frequencies. Two radial and nonradial linear theory pulsation programs have been developed by Pesnell (1988) using a Lagrangian mesh and using a solution method described by Castor (1971) for the radial nonadiabatic case. The second smaller program gives only adiabatic solutions for nonradial cases, but it has more elaborate inner boundary conditions. This second program has also been used for the radial adiabatic and nonadiabatic modes. Comparisons of p-mode frequencies between both the eigensolution programs shows that the two different inner boundary conditions affect values by less than 1 μHz. The agreement for the g-modes at $l = 2$ is better than 1 μHz in 200 for the low-order modes, where the different boundary conditions show the most sensitivity.

The outer mechanical boundary condition has been tested to

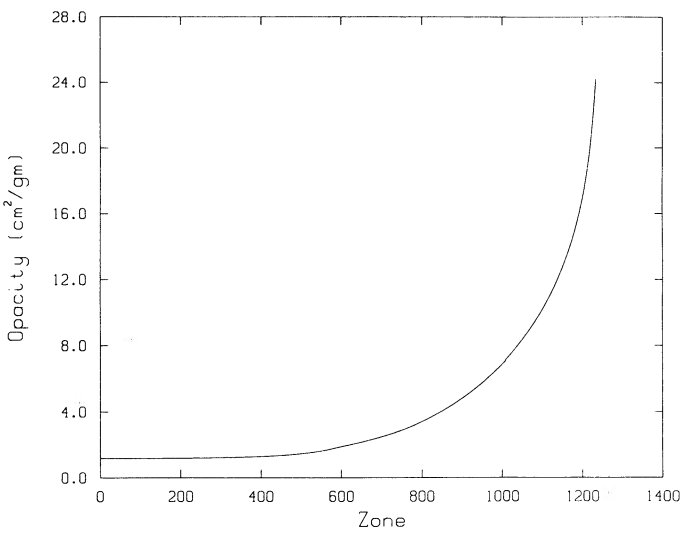

FIG. 5

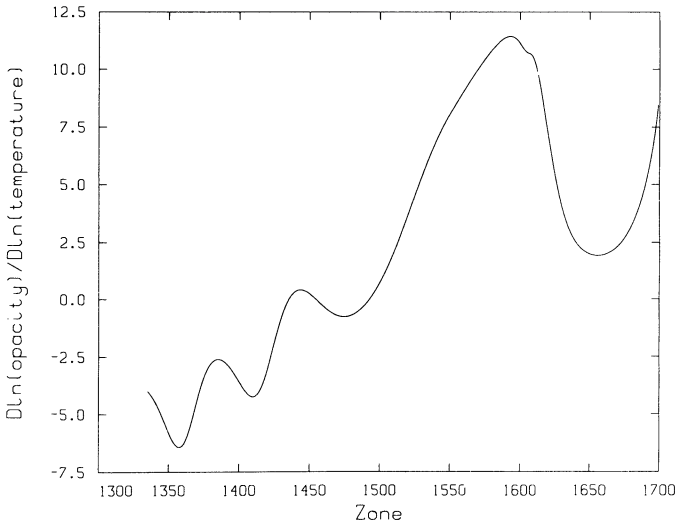

FIG. 6

FIG. 5.—Opacity in the no-diffusion model is displayed vs. the zone number for those zones below the convection zone. The central opacity 1.16 $cm^2\ g^{-1}$ is caused by electron scattering, free-free absorption of photons in the fields of hydrogen, helium, and the CNONe ions, and the bound-free absorption by almost completely ionized iron.

FIG. 6.—Logarithmic derivative of the opacity with respect to the temperature is plotted vs. zone for the no-diffusion model. The large positive derivative at the surface is caused by the rapid increase with temperature of the hydrogen bound-free absorption. The rapidly increasing ionization gives another hydrogen opacity peak near 1.1×10^4 K near zone 1600. The peak at zone 1450 at 4×10^4 K is caused by the helium ionization. The deepest lying peak in the model is the Stellingwerf (1978) "bump" near 1.2×10^5 K, and it is only 3% of the radius into the stellar model. The opacity derivative with respect to temperature remains negative the rest of the way to the center, causing only radiative damping and no driving for any pulsations.

see its effect on p-mode frequencies and decay rates. A change in the inertial mass from 7.7 to 1.0 times the last mass shell mass in the eigensolution results in less than a 2 μHz change for the $l = 100$, p_6 mode, but the decay rate is affected by almost 30%. One can see that if extreme accuracy is needed in these quantities, very careful program development will be necessary.

The Lagrangian variation of the convection luminosity both horizontally and radially has been set to zero for the eigensolutions given here. This freezes in the convection luminosity, which is not a bad approximation if the time scale for its change is long compared to the pulsation periods under consideration. This technique was developed because the energy equation needs to cope with the convection luminosity gradient with mass level in the model. The often-used zeroing of the divergence of the convection luminosity leads to terms which involve the convection luminosity gradient, and to artificial damping or driving terms. Our method is very similar to that used by Ando and Osaki (1975).

It appears that the 300 s p-modes are driven by coupling to the 300 s time scale convection at the top of the convection zone. This forcing due to the coupling to granular convection, as well as the effects of convective luminosity variations, are not included in these calculations.

The influence of the luminosity on the p-mode frequencies has been studied by using two luminosities differing by 0.94%. The $l = 2$ and $l = 200$ p-modes differ by less than 1 μHz, with the higher luminosity giving lower frequencies. The differences grow with mode order, reaching 1 μHz at just over 4000 μHz for $l = 200$. They are smaller for $l = 2$, as expected, because these lower degree modes feel less the surface conditions that are affected by the change in luminosity. Thus we might predict that as the solar luminosity increases going into the next solar cycle, the p-mode frequencies might decrease by a fraction of a microhertz. However, the observations in the last few years during which the luminosity was decreasing may indicate the opposite effect. Brown (1987*b*) and Jefferies *et al.* (1988) suggest that the p-mode frequency changes may be much smaller than other authors have suggested.

Changes in the p-mode frequencies may reflect only cyclical changes in the structure in the very outer part of the convection zone. The depth into the Sun where the luminosity times the solar activity cycle period (about 10^{41} ergs) equals the internal energy from there to the surface is only at a temperature of about 10^5 K and has only 10^{-5} of the solar mass. Nonadiabatic effects, which are several microhertz typically, could change slightly as the convection zone adjusts during the solar cycle. The observed p-mode frequency changes are most likely only a probe of the convection zone upper layer structure.

The comparison between our theoretical adiabatic and nonadiabatic oscillation frequencies for the no-diffusion model and those observed is given in Figure 8 for low-l modes. Figure 9 shows this comparison for the same modes for the model where diffusion is allowed to separate the elements. One can see that the nonadiabatic effects reduce the slope of the $O - C$ (observed minus calculated) curves nearly to zero, but there remain a few microhertz differences from observed frequencies. The effects of the diffusion make the agreement poorer, but that is not entirely unfortunate because we feel that our diffusion calculation has indeed overestimated the element separations. Figure 10 gives the same comparisons for higher l values in the no-diffusion case, showing that our equation of state problems in the convection zone do really affect the $l = 200$ modes.

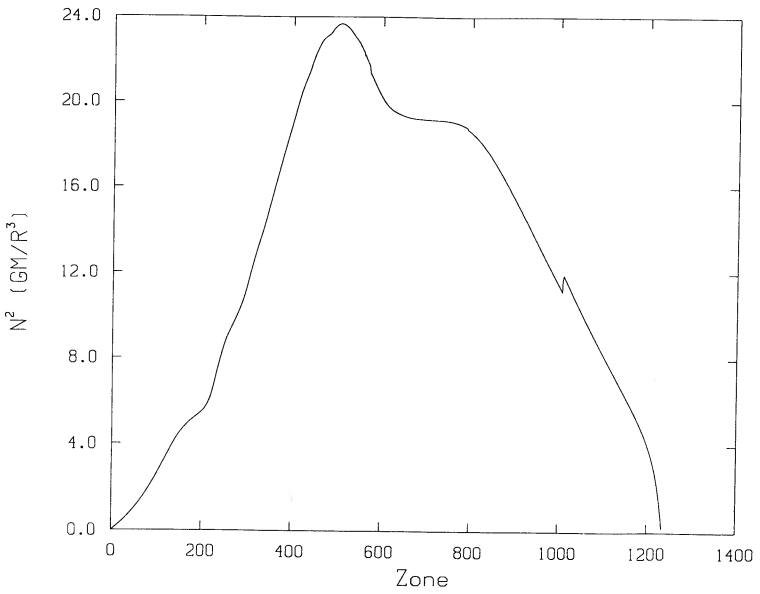

FIG. 7.—The square of the Brunt-Väisälä frequency is plotted vs. zone number for the no-diffusion model. The unit is the natural one, GM/R^3. The peak at 1.3×10^7 K and 0.1 of the mass from the center is due to a combination of a very subadiabatic temperature gradient and a steep composition gradient. The shoulder between zones 600 and 800 is caused by the interplay of a less steep composition gradient halfway out in mass of the model and the increasing degree of subadiabaticity of the temperature gradient toward the surface out to zone 800. The switch from the Iben ionization procedure and complete ionization at 4.5×10^6 K is seen by the small notch near zone 1000. Slight variations in the composition gradient because of our spline fit to the evolution program data at 1.5×10^7 K give small ripples in the Brunt-Väisälä frequency at the center.

Comparison between the $O-C$ plots for the no-diffusion and the diffusion cases shows that the allowance for diffusion makes the $O-C$ about 3 μHz larger. This may be caused by the shallower convection zone when diffusion was considered.

The tendency for the $O-C$ to get larger at higher frequency may be due to the overestimate of the nonadiabatic effects there. We get very rapid decay rates using only radiation luminosity modulation. but if there is some pulsational driving from the sidewise flow of convective luminosity in the superadiabatic region (Cowling effect, see Unno *et al.* 1979; Antia, Chitre, and Narasimha 1982) that we here neglect, the decay rates will be smaller, and the nonadiabatic frequency decreases will be smaller.

The agreement between theory and observations for these p-modes is as good as or better than the most relevant recent models by Christensen-Dalsgaard (1982; see Christensen-Dalsgaard and Gough 1984), by Shibahashi, Noels, and Gabriel (1983), by Scuflaire, Gabriel, and Noels (1984), or by Bahcall and Ulrich (1988). The first of these has $O-C$ frequencies positive at low frequency and negative at high frequency. The second often has agreement better than 5 μHz, but use of nonadiabatic frequencies would make the agreement worse. The third has $O-C$ negative over the whole 5 minute band, while the last has $O-C$ positive over the whole band. In these last three cases, only low-l values were used. Better agreement of our frequencies might have been produced if we had used an even higher opacity in the few million kelvin temperature region, requiring an even larger initial helium abundance to match the observed luminosity.

The $O-C$ varies with frequency and radial order. If the frequency is fixed, higher l values produce a turning point in the motions nearer to the surface, allowing only lower radial order modes to exist. But for these modes, the surface lobes all have almost the same shape and sample the convection zone the same way. However, at higher frequency, the modes have more radial nodes and sample the convection zone at least in a different way than for lower frequency and order modes. Thus the $O-C$ plots could, in principle, map the errors in our convection zone structure.

An earlier version of this paper presented $O-C$ plots of the p-mode frequencies calculated from models without the Coulomb effects in the gas pressure and energy. Then the $O-C$ values were 10 μHz–20 μHz larger, a finding similar to those of Shibahashi, Noels, and Gabriel (1983) and Stix and Knoelker (1986).

A widely used quantity for measuring the central solar structure is

$$\delta(n) = \nu_{n,0} - \nu_{n-1,2} ,$$

with n the radial order of the mode and the second subscript being the l value of the spherical harmonic function. Since the radial and quadrupole modes penetrate deeply into the Sun but are similar to each other in the outer regions, their frequency difference (or ratio) is indeed sensitive to the solar center, as pointed out by many before (Faulkner, Gough, and Vahia, 1986; Däppen, Gilliland, and Christensen-Dalsgaard 1986). Figure 11 gives $\delta(n)$ versus mode order for the two models using nonadiabatic frequencies. These nonadiabatic frequencies are typically a few microhertz smaller than the adiabatic ones (see Kidman and Cox 1984 for quantitative nonadiabatic period increments), but understandably the nonadiabatic frequency decrease, set right at the top of the convection zone, is almost the same for the two modes being subtracted. Thus the differences between the adiabatic frequencies is the same as those plotted to within 0.1 μHz. Also plotted in the figure are the observed differences of the mode frequencies (Jiménez *et al.* 1988), and an asymptotic theory line

(for the no-diffusion case) using the formula (Tassoul 1980):

$$\delta(n) = 6Av_0/(n+1)\,,$$

where

$$Av_0 = \left[\frac{c(R_\odot)}{R_\odot} - \int_0^{R_\odot} \frac{dc}{dr}\frac{dr}{r}\right] \Big/ 4\pi^2\,,$$

and

$$v_0 = 1 \Big/ \left[2\int_0^{R_\odot} (dr/c)\right].$$

Here c is the sound velocity. The integrals Av_0 for the no-diffusion and diffusion models are 38.8 and 39.3 μHz. The corresponding v_0 values are 139.0 and 138.9 μHz.

The agreement with asymptotic theory gets better for higher order, as it should. However, most workers have found closer agreement with asymptotic theory than we have at these orders. Recent discussions of the asymptotic theory by Smeyers and Tassoul (1987) do not change the above comparison. We suspect that (1) the decrease of the sonic velocity with radius at the solar model center (due to the high-temperature gradient set by the high opacity) followed by (2) a frequently seen increase further out, an finally (3) a decrease way out to the surface may produce gradients that are too severe for the asymptotic theory. An indication that the theory is not exactly valid for our models is that the v_0 also is calculated to be too large at 139 μHz, whereas the separation between the actually calculated frequencies is nearer 135 μHz.

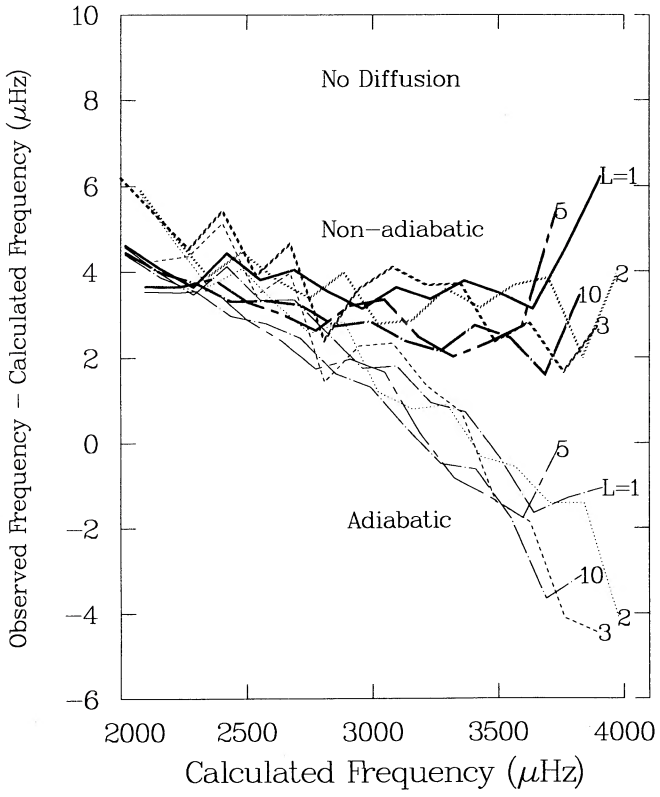

FIG. 8.—$O-C$ p-mode adiabatic and nonadiabatic frequencies are plotted vs. the frequency for the no-diffusion model. These $l = 1$–10 modes sample mostly the model region below the convection zone. Broken curves reflect errors both in the observations and the theoretical predictions.

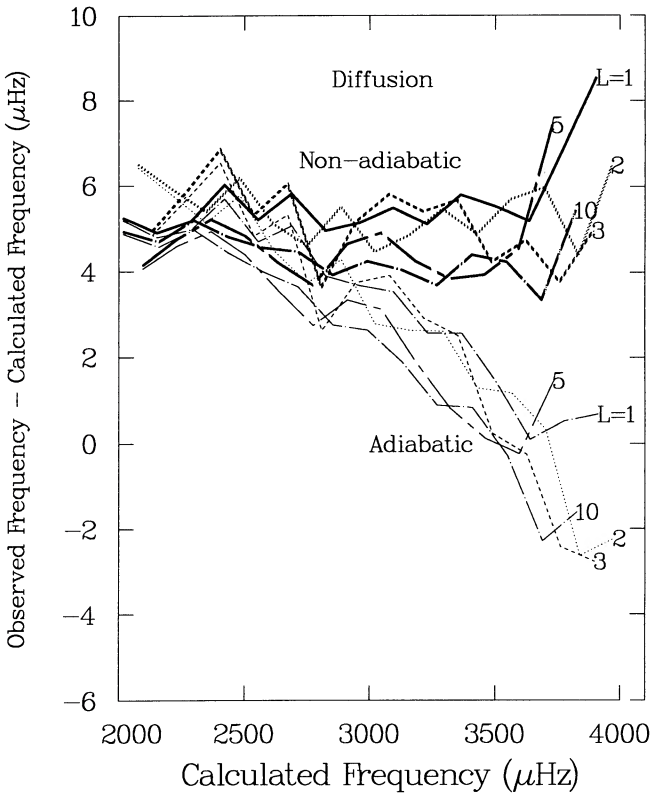

FIG. 9.—$O-C$ p-mode adiabatic and nonadiabatic frequencies are plotted vs. the frequency for the diffusion model. These $l = 1$–10 modes sample mostly the model region below the convection zone.

Other solar models calculated by us that do not have such a high central opacity show a more close agreement between the $\delta(n)$ from asymptotic theory and frequencies calculated in detail. Thus one can sometimes but not always rely on the applicability of asymptotic theory.

A similar plot of the frequency splittings for different models has been presented by Lebreton, Berthomieu, and Provost (1986). For their models, however, the $\delta(n)$ values run about 2 μHz larger for their mixed model and ~ 1 μHz larger for their standard one.

The agreement with observed frequency differences, at least at low order, suggests that we do not need to invoke any special cooling mechanism, such as weakly interacting, massive particles (WIMPs), for the solar center (see Faulkner and Gilliland 1985). In two papers (Faulkner, Gough, and Vahia 1986; Däppen, Gilliland, and Christensen-Dalsgaard 1986) it was pointed out that a cooler central temperature and a denser core, with not much change in the central composition, would give a lower central temperature and therefore a lower neutrino production rate. The lower temperature also would result in a lower sonic velocity. This then gives a lower Av_0 and a lower $\delta(n)$, which seemed to agree better with observations. The first of these papers did not involve actual period calculations, and the possible inapplicability of asymptotic theory to high precision (see Fig. 11) causes their calculated $\delta(n)$ to be a bit too large. The second paper, with actually calculated low-degree p-mode frequencies, does not strongly

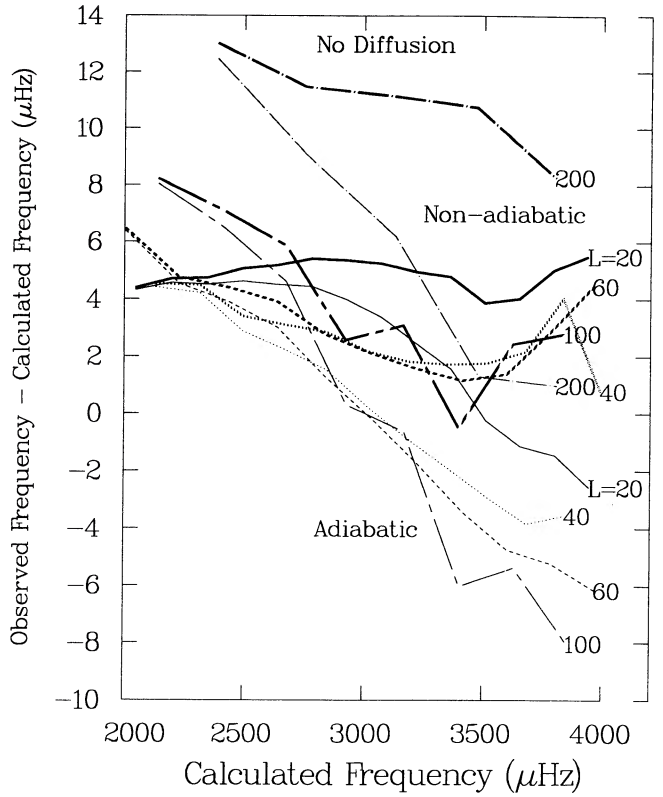

FIG. 10.—$O-C$ p-mode adiabatic and nonadiabatic frequencies are plotted vs. the frequency for the no-diffusion model. These $l = 20$–200 modes sample mostly the convection zone and do not show the small increase in $O-C$ that the deeper penetrating lower degree modes do.

support or refute an unconventional central cooling. Our p-mode results, with better agreement between theoretical and observational frequency differences, do seem to refute the existence of extensive cooling of the solar center by WIMPs.

This conclusion is in direct conflict with the recent result of Gilliland and Däppen (1988), who find support for WIMPs in the p-mode differences. A possible explanation is that the opacities (Cox and Stewart 1965) used by these authors are lower than those from the latest Los Alamos calculations. They are certainly lower than our arbitrarily increased values at $2–7 \times 10^6$ K. There may also be equation of state differences between their calculations and ours.

A recent discussion of the observations has been made by Gelly *et al.* (1988), who point out that theoretical $\delta(n)$ frequency differences from standard models, such as ours, agree well with observations. Further discussion on this question is clearly needed.

The agreement between observations and theory for $\delta(n)$ at the highest frequency is not satisfactory. Perhaps it is due to observational error. It does not seem possible that our larger than correct helium abundance could be the problem, because a decrease of 0.02 in Y would produce only a 1% increase in the sonic velocity everywhere and a 1% increase in $\delta(n)$.

One can speculate that the larger $\delta(n)$ for the deepest penetrating modes reflects an even higher central sonic velocity. Such a high sonic velocity might be the result of a larger central temperature (our central opacity from the Iben procedure needs to be slightly increased) or more central hydrogen (and therefore a higher sonic velocity) than we have in our models produced by a mixing event in the past. Of course, too much hydrogen would upset the luminosity that has been matched to the present solar value. If the observations are correct, the discrepancy points to a fascinating probe of the central few percent of the solar mass.

The variations of $\delta r/r$, $\delta h/r$, and the weight (Pesnell 1988) for determining the period for the diffusion model are given in Figures 12–14 for the p_6-mode with $l = 100$. Especially in the weight plot, one can see that the structure of the solar convection zone is essential for accurately predicting the p-mode frequencies. If a scaling by $r\sqrt{\rho}$ were used, as discussed by Christensen-Dalsgaard (1984), the amplitudes of the radial and horizontal motions would not drop off so fast with depth. The ratio of the surface horizontal to radial amplitudes is close to 10^{-3}, as expected from the equation given by Cox (1980), but the actual horizontal motions are l times larger than plotted for these $m = 0$ zonal modes.

Modulation of the radiation flow produces some κ and γ effect driving just at 9000 K at the top of the convection zone, but exterior to that point there is radiation damping. The relative amount of driving and damping depends greatly on the temperature and density derivatives of the opacity, and with the Stellingwerf fit adjusted by a factor of 3, as described above, some net pulsation driving is found for this mode. Use of the King IVa table of Cox and Tabor (1976) or the unadjusted Stellingwerf (1975a, b) fit produces damping of this mode, as

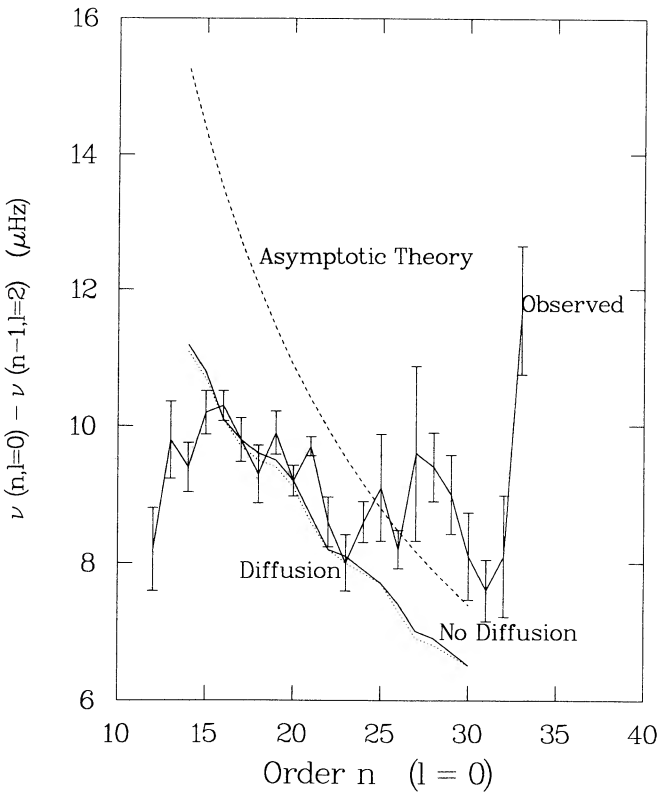

FIG. 11.—The $\delta(n)$ nonadiabatic frequency difference between the radial and quadrupole modes for radial orders 14–30 is plotted vs. radial mode order for the no-diffusion and diffusion models. Agreement with observations is seen for low orders only, whereas our $\delta(n)$ approaches asymptotic theory only at very high order.

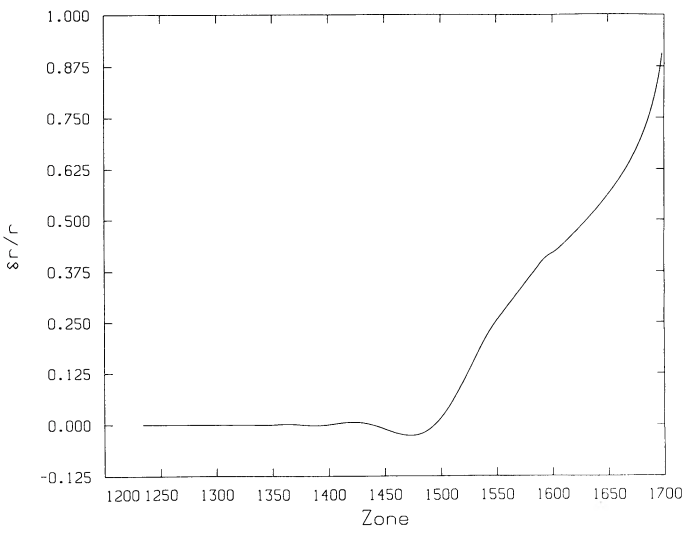

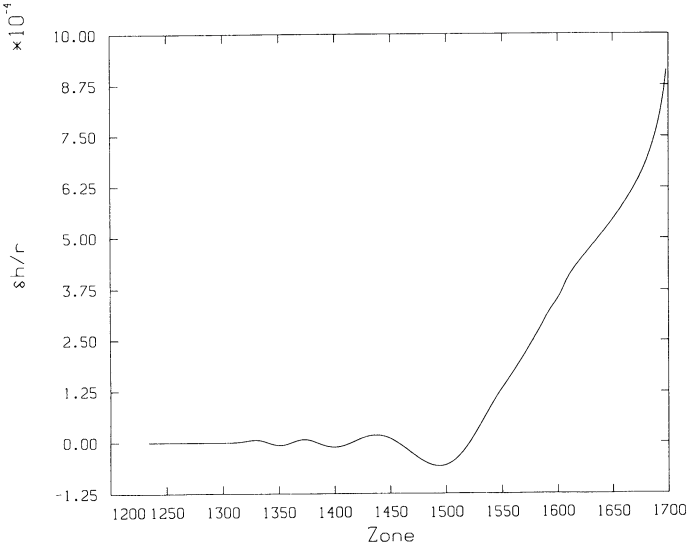

FIG. 12.—The real part of the variation of the radial motions in the no-diffusion model is plotted vs. zone number for the p_6-mode with degree $l = 100$. All six nodes are exterior to the bottom of the convection zone at zone 1234; deeper, the mode is evanescent.

FIG. 13.—The real part of the variation of the small horizontal motions in the no-diffusion model is plotted vs. zone number for the p_6-mode with degree $l = 100$. The true horizontal motion is l or 100 times larger. All six nodes are exterior to the bottom of the convection zone at zone 1234; deeper, the mode is evanescent.

reported by Kidman and Cox (1984). Even though their low-degree mode damping seems to accord well with the measured lifetime of modes from their line widths in the Fourier spectrum, there must be some driving or the modes would never be observed. We suggest that there are brief episodes of convection-coupled driving to excite the modes, but the damping we calculate each cycle occurs continuously over the life of each manifestation of a mode.

We get pulsational instability for the p-modes in the Sun which depends greatly on the opacity derivatives with respect to temperature and density. The fact that Ando and Osaki (1975) and Goldreich and Keeley (1977) get pulsational instability in nonadiabatic calculations from the κ-effect depends greatly on several things, including the accuracy of their opacities. The former authors used the Paczyński (1969) opacity formulation, whereas the later ones have used the Christy (1966) fit. We find a great sensitivity to opacities and have found that the King IVa opacity table seems to have the opacities that best fit the slowly decaying p-modes. Only when other effects such as the turbulent viscosity and time-varying convection are considered, as well as the actual radiation transport structure of the subphotospheric layers, will accurate stability calculations be possible for the solar p-modes.

An interesting question concerns the maximum l-value of p-modes in the Sun. Such modes would have lifetimes equal to their frequencies. We do not have a definite answer to this question, but at $l = 1400$, the 5 minute p-modes have decay rates approaching 10% per period. We guess that any $l = 2000$

TABLE 7

SAMPLE g-MODE RESULTS (FOR $L = 2$)

Number of G-type Nodes	Nonadiabatic Frequency (μHz)	Work Integral Growth Rate (e cycle^{-1})	Total Kinetic Energy (ergs)	Photospheric $d(\ln T)$	$\frac{dT/T}{(\mathrm{KE})^{1/2}}$
15	74.3	−1.9E−08	4.5E+49	2.5E+00	3.7E−25
14	79.2	−1.5E−08	3.3E+49	2.3E+00	4.0E−25
13	84.8	−1.2E−08	2.3E+49	2.1E+00	4.3E−25
12	91.3	−9.3E−09	1.5E+49	1.9E+00	4.8E−25
11	98.5	−7.4E−09	1.1E+49	1.7E+00	5.2E−25
10	106.9	−5.7E−09	7.7E+48	1.5E+00	5.5E−25
9	116.4	−4.5E−09	6.0E+48	1.4E+00	5.7E−25
8	127.7	−3.5E−09	4.7E+48	1.3E+00	5.9E−25
7	140.9	−2.6E−09	3.7E+48	1.2E+00	6.2E−25
6	157.2	−1.8E−09	2.6E+48	1.1E+00	6.8E−25
5	176.9	−1.2E−09	1.5E+48	1.0E+00	8.3E−25
4	200.9	−7.1E−10	8.0E+47	9.9E−01	1.1E−24
3	228.6	−3.3E−10	4.4E+47	9.7E−01	1.5E−24
2	263.0	−5.3E−11	3.1E+47	9.7E−01	1.7E−24

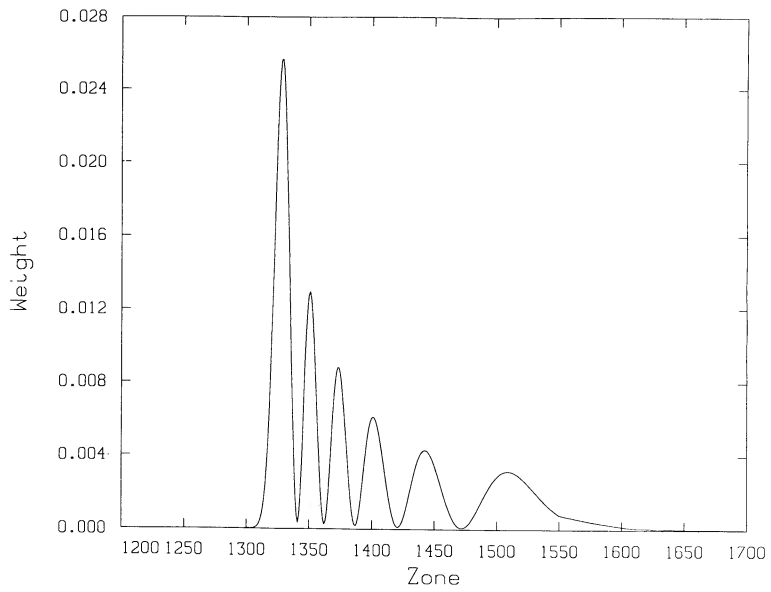

FIG. 14.—Weight for determining the oscillation frequency is plotted vs. mass zone number in the convection zone. Note that the six peaks for this p_6-mode with degree $l = 100$ sample the entire convection zone, but considerable weight is concentrated close to the bottom at zone 1234.

p-mode would be difficult to detect, not only because of its small spatial size, but because its lifetime is so short.

VI. *g*-MODE FREQUENCIES

For the calculation of the *g*-mode eigensolutions, the standard Castor (1971) method for the matrix inversion often fails because the method becomes nearly singular. That is because the right-hand side vector in the Castor formulation contains the surface part of the matrix information, and for these *g*-modes it is almost zero when the main part of the eigenvector is deep in the model. In that case the method of inverse iteration (Golub and Van Loan 1983, p. 238; Keeley 1977) for the eigenvector is used with an approximate eigenvalue, and then, with the calculated highly accurate eigenvector, the eigenvalue can be easily obtained.

Our theoretical frequencies for *g*-modes of degree $l = 2$ (and, of course, $m = 0$) are given in Table 7, as well as the negative kinetic energy growth rates, kinetic energies (for this unity real and zero imaginary part surface displacement), and unscaled and scaled photospheric temperature amplitudes. According to Hill and Gu (1988), observed frequencies for $l = 2$ are 4–9 μHz smaller for orders 6–15. Data from Severny, Kotov, and Tsap (1984) for $l = 4$ show that we have predicted periods 20–30 minutes too short, that is, our frequencies are 15% too high. Additional data are given by Kotov *et al.* (1984) and Pallé and Roca Cortés (1986), as reported by Fröhlich (1986), but we have not tried to discuss the data which are based on identifications that assume the *g*-modes are equally spaced in period. Also we have not considered the data by Delache and Scherrer (1983), who use equal period spacings for identifications with this spacing scaled by $\sqrt{l(l+1)}$ being 38.6 minutes. One can easily see that there is little correspondence between many of the claimed *g*-mode frequencies, leading one to suspect that the data may not be correct.

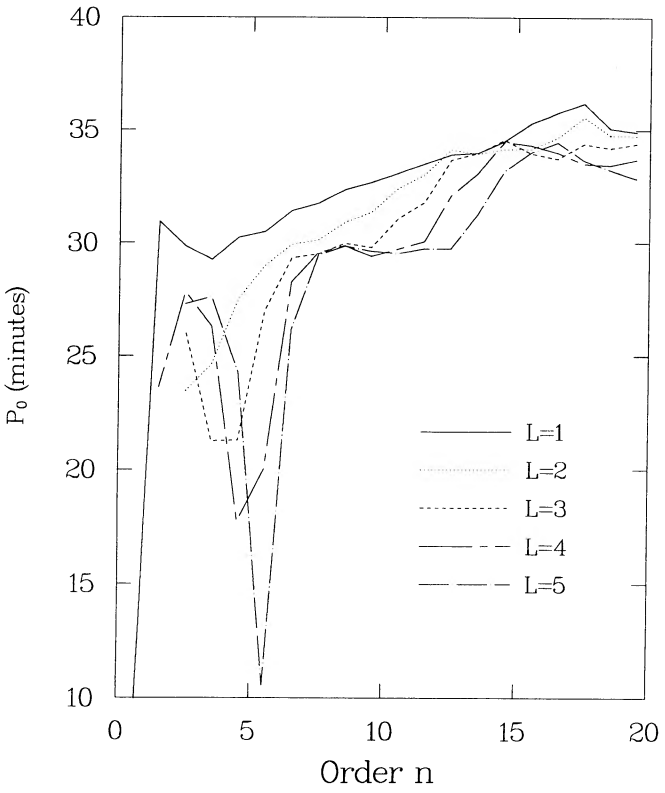

FIG. 15.—Period spacing between mode periods multiplied by $\sqrt{l(l+1)}$ is plotted vs. *g*-mode order for $l = 1$–5. Fluctuations at the low order are caused by mode "bumping" as discussed in the text. The lowest degree modes reach the asymptotic region at the lowest order, and this P_0 is somewhat larger than the $P_0 = 34.3$ minutes calculated from the no-diffusion model as discussed in the text. Our lack of high accuracy in the period determinations, due to the coarse mesh at the very center of the model, begins to affect the calculated period spacings even before order 20.

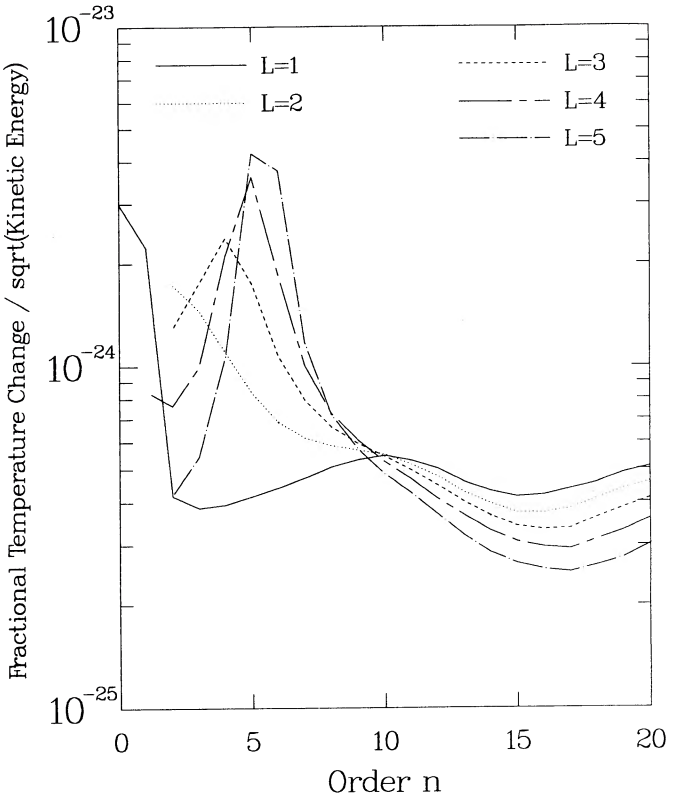

FIG. 16.—Fractional temparature amplitude per unit square root of the kinetic energy is plotted vs. g-mode order for $b = 1$–5.

Our frequencies also run high relative to those theoretical ones plotted by Christensen-Dalsgaard (1986) and those tabulated by Gabriel (1984). In this latter case our $l = 2$ frequencies are 5% higher. These differences are not caused by nonadiabatic effects, because, with such small decay rates, the adiabatic and nonadiabatic periods agree to at least one part in a million. The differences are compatible with our integral for P_0 (see below), being also about 5% too low relative to the value for most current solar models. They are probably caused by the central density being higher than usual when using the somewhat larger central helium. Our more concentrated model will always give higher pulsation frequencies.

Comparisons with the iron-like core model g-mode data of Rouse (1985) show that his Cowling approximation periods are much lower than ours, but perhaps there should not be much agreement expected between such greatly different models.

The spacing between these g-mode periods should have a value $P_0/\sqrt{l(l+1)}$ for high order, where (in units of seconds if N is in cycles s^{-1})

$$P_0 = 2\pi^2 \Big/ \int_0^{r_c} \left(\frac{N}{r}\right) dr \, .$$

Here N is the Brunt-Väisälä frequency that is positive only out to r_c, the radius of the convection zone bottom. The integrals for the no-diffusion and diffusion models are 34.6 and 34.5 minutes, respectively, with possible integration uncertainties of less than a few percent. Because of our higher central helium and central temperature, this value is smaller than that obtained for many recent solar models. Our gradient at the solar center is more subadiabatic than usually calculated. This effect, and the composition gradient just below the convection zone, makes the Brunt-Väisälä frequency higher than obtained previously both at the center and near the bottom of the convection zone of our diffusion model.

Figure 15 shows the scaled period spacing for our g-modes versus order for the first five l values; one can see that the asymptotic value is not reached until moderate order. Thus low-order observations of g-mode period spacings are not likely to be easily used to measure the central solar conditions because the periods are not evenly spaced. For an asymptotic theory analysis of this phenomenon see Provost and Berthomieu (1986). This increase of period spacing with radial order was apparent from results from as long ago as Iben and Mahaffy (1976). Also note that the spacings are not always smoothly increasing with order because of the phenomenon of avoided crossings. For the Christensen-Dalsgaard (1982) Model 1, this g-mode bumping can be seen in the plot of frequency verus l given by Christensen-Dalsgaard (1986).

Even though we have used a mass mesh in the central regions with more resolution (except right at the center) than that kindly sent to us by Christensen-Dalsgaard in his g-mode determinations, the accuracy of our g-mode periods is only approximately one part in 1000. Thus with the spacing between periods of 5%–15% for orders 1–20 with $l = 1$, and with much less spacing for the higher l-values, the P_0 accuracy for higher order modes grows to a few percent. This can be seen by the unphysical P_0 variation in Figure 15. Reliance on the Provost and Berthomieu results is necessary for higher order g-modes.

The most recent determination of P_0 is by Barry *et al.* (1987), where the value fit to asymptotic theory is 36.25 minutes. This value is based on 53 g-mode multiplets classified by n, l, and m values. The value of 29.85 by Fröhlich (1986) seems incorrect, even though, for his high-order modes, the asymptotic approximation seems to be accurate enough.

It appears from the g_{10} $l = 2$ mode (possibly the famous 160 minute mode, although some think that the mode may have $l = 3$ or that there is not even a solar oscillation mode at all) that our predicted g-mode frequencies are too large by several percent. This might be expected if our Brunt-Väisälä frequency is systematically too large throughout the deep interior because of our high helium abundance and high central temperature. Our systematically higher pressure gives higher helium and therefore requires a higher central temperature to obtain the solar luminosity.

There is the controversial question as to whether the g-modes that Hill and collaborators report are really visible on the surface. Hill, Tash, and Padin (1986) have discussed this visibility problem and conclude that their observable quantity is the photosphere temperature variation as opposed to limb motions. Thus it is interesting to plot the temperature variation amplitude at the photosphere for these g-modes. Such data could be obtained very approximately from adiabatic eigensolutions of the pulsation equations, but here we use the nonadiabatic solutions because there are important nonadiabatic effects right at the photosphere. Figure 16 shows that there is a great variation in visibility from mode to mode, assuming that all modes have the same kinetic energy. There is a tendency for the lower order modes to have larger amplitudes for equal energy of the mode, however, as one can see by looking at the

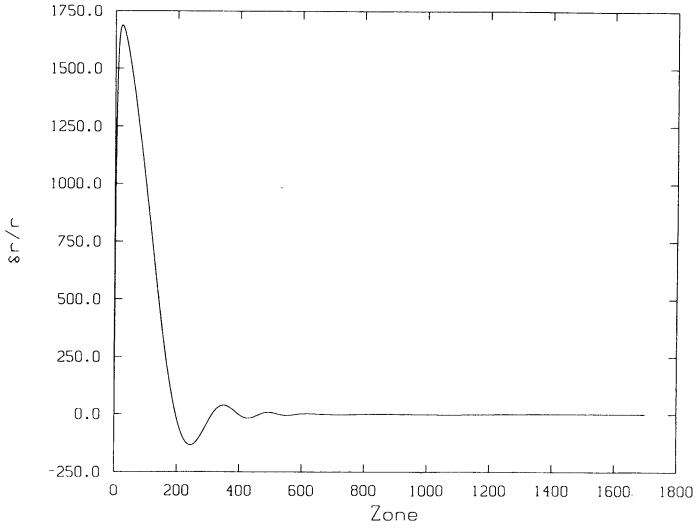

FIG. 17

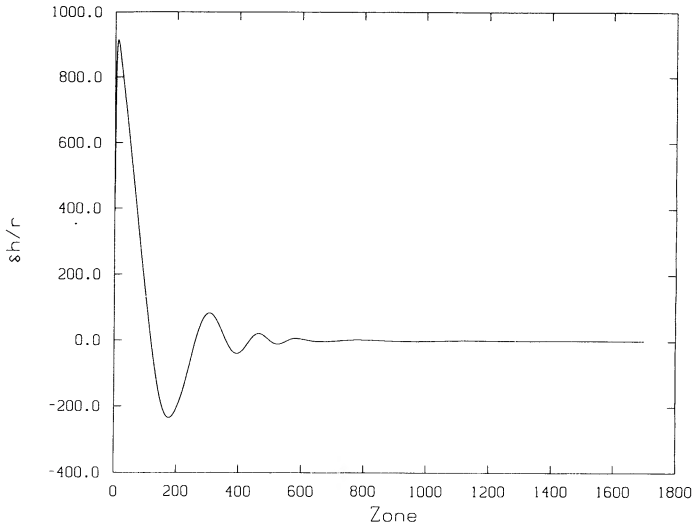

FIG. 18

FIG. 17.—The real part of the variation of the radial motions in the no-diffusion model is plotted vs. zone number for the g_{10}-mode with degree $l = 2$. Only six of the 10 radial nodes can be easily seen, and they are in the central 15% of the radius. The mode is evanescent in the convection zone for mass shells exterior to zone 1234. Note that with the normalization scale of unity amplitude at the surface, the amplitude at $\sim 0.5\%$ of the radius and 10^{-4} of the mass from the center is over 1600. This is the neutrino-producing region near 1.57×10^7 K and at a density of about 162 g cm^{-3}.

FIG. 18.—The real part of the variation of the horizontal motions in the no-diffusion model is plotted vs. zone number for the g_{10}-mode with degree $l = 2$. Only six of the 10 radial nodes can be easily seen. The mode is evanescent in the convection zone for mass shells exterior to zone 1234. Note that with the normalization scale of unity amplitude at the surface, the amplitude at $\sim 0.5\%$ of the radius and 10^{-4} of the mass from the center is over 900. The actual horizontal motions are $l = 2$ times larger.

last column of the data in Table 7. Of course, a particular mode may have been excited somehow a short time ago, and thus it will be much more prominent than those that have decayed already or were never excited at all.

Figures 17–20 give the variations of the radial and horizontal motions, the work per zone per cycle, and weight for the period as a function of zone number for the g_{10} mode with $l = 2$. As expected at this period, the surface radial and horizontal amplitudes are about equal, and this equality persists approximately throughout the entire model. Note that even though the weight function becomes negative for this g-mode because it is the derivative of the usually discussed function (Pesnell 1988), its integral still produces very closely the period determined from the eigenvalue of the eigensolution. This reasonably visible mode does have large radial and horizontal amplitudes in the deep layers, which might influence the neutrino production.

Note that radiative damping of the mode, which is due to radial heat flow, amplified by the large horizontal motions giving temperature and density variations, occurs throughout the interior, with just a bit of periodic convection blocking pulsational driving (Cox *et al.* 1987; Pesnell 1987) at the bottom of the convection zone. In some of our solar models, but not those reported here, for low-order $l = 1$ g-modes, this convection blocking produces unstable and observable modes. However, there probably is convection damping near the surface where the turnover time is approximately the g-mode period, because the g-modes are not seen at large amplitude in the Sun. Even if there is g-mode pulsation driving, the observed low surface amplitude may be due to an amplitude limitation from nonlinear effects, such as those that limit amplitudes of classical variable stars.

The central regions display just a slight amount of p-p burning ϵ-effect pulsation driving at the five peaks in the center out to zone 450. The temperature at this coolest point for the ϵ-effect is 14×10^6 K. CNO cycling has changed most of the carbon to nitrogen in these deepest layers, but no ϵ-effect would be expected from that cycling anyway for the present Sun. The peak of the ^{3}He abundance is at zone 784 at an interior mass fraction of $q = 0.57$, and no ϵ-effect is seen there where the temperature is just over 7.2×10^6 K.

Radial heat flow variations produce maxima in the pulsation damping at levels in the model where the radial motions on opposite sides of a node line are at maxima. This gives rise to a small Cowling effect that causes damping. Since the local temperature gradient is subadiabatic, a rising element gains heat from the falling element across a node line, and its cycling in the P-V plane is counterclockwise giving damping of this element's motion.

Even though there is net damping in the model for this g_{10}-mode, it is small compared with the kinetic energy of the mode. Thus the decay rate is slow for any small perturbation of the model in this mode. With a lifetime of over 5×10^4 yr, it is not surprising that all observers agree on the phase of this mode.

The weight for the period determination is greatest near the center, holding open the possibility that the solar center can be diagnosed if reliable g-mode frequencies are measured.

Hill (1986) discusses possible mode-locking in the $l = 30$, g_{15}-mode among the various m-values. We have calculated this mode and find that the amplitude oscillations all occur between zones 300 and 900, with the peak near zone 400 in our no-diffusion model. This is expected because this high-order mode would have a frequency just under the Brunt-Väisälä frequency peak. It seems unlikely, however, that this mode would be visible at the solar surface, because the radial

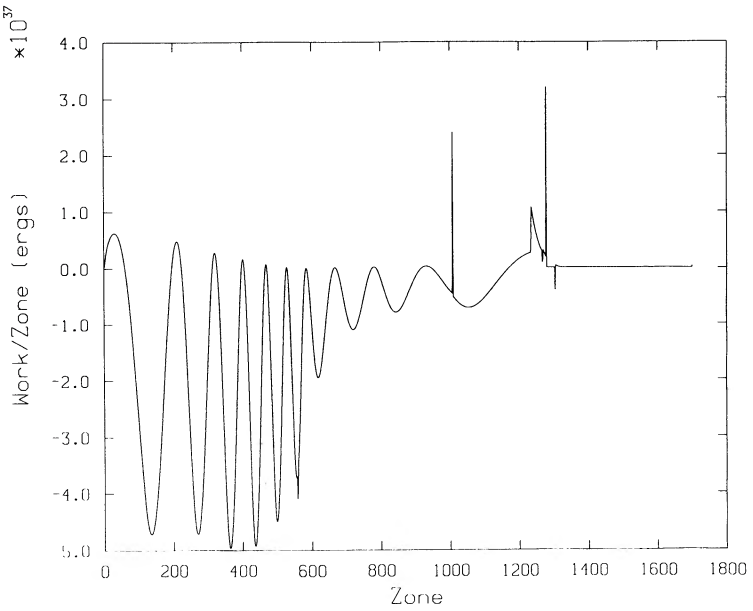

FIG. 19.—Work over each pulsational cycle is plotted for each zone for the g_{10}-mode with degree $l = 2$ in the no-diffusion model. Some pulsational driving occurs at the bottom of the convection zone, where the periodic flow of radiative luminosity is blocked by relatively slowly changing convection, as found also in the white dwarfs. There are 10 peaks in the deeper work per zone, with the bottom five displaying the nuclear energy modulation (ϵ) effect driving. The switch to more realistic composition due to partial CNO cycling can be seen near zone 580 (1.2×10^7 K), and the Iben opacity switches to different approximations at zones 1304 (10^6 K) and 1278 (1.5×10^6 K) can be seen also. The complete ionization switch is at zone 1008 (4.5×10^6 K). Small errors in the convection zone structure result in work excursions at zones 1268 and 1310. The net damping gives the mode theoretical lifetime of about 1.8×10^8 cycles, that, at a period of 9354 s (107 μHz) is over 5×10^4 yr.

motions are almost 10^{10} times larger at zone 350 (at about 15×10^6 K) than they are at the surface. Further, the temperature variations are almost 10^8 larger there than at the surface, making a fraction of degree variation at the surface essentially a 100% temperature variation in the neutrino-producing layers. We suggest that this mode has not really been detected.

VII. DISCUSSION AND CONCLUSIONS

The present solar structure is determined in this work by fitting the solar mass, radius, luminosity, age, and observed p-mode oscillation frequencies. The effects of diffusion reduce the surface helium and Z values such that the arbitrarily assumed Z-value seems to evolve to the present observed value of about 0.018. Apart from a problem of our pressure values from the equation of state that artificially require a small excess of helium, we feel that matching the observed solar parameters is now about the best that one can do.

If the primordial big bang helium abundance Y is 0.24, and if the solar value is 0.29 or maybe only 0.28 in order to correct for our equation of state problem, the galactic enhancement has been about 0.04 or 0.05. Studies show that observed Y-values in various objects range between 0.18 and 0.28 (Boesgaard and Steigman 1985), and thus our value $Y = 0.29$ is near the maximum allowable. With a Z enhancement of 0.02, we can see that the $\Delta Y/\Delta Z$ ratio is 2.0 or even 2.5 (Peimbert 1986). Such a ratio seems reasonable, but one should remember that metals are created in massive short-lived stars, whereas the helium comes from lower mass stars, with the time to create and lose the helium being a good fraction of the lifetime of our Galaxy. Nevertheless, it seems that the Sun, being a later generation star, should see both enhancements, as we seem to require.

There is a problem of the lithium abundance being apparently about a factor of 20 less than seen in younger solar mass stars. The temperature at the bottom of the convection zone varies in the diffusion model from 2.47×10^6 K at 4×10^8 to 2.14×10^6 K at the present age. Enough lithium would be destroyed if a temperature of more than 2.5×10^6 K were maintained for a billion years, but our diffusion model does not remain at that temperature for long enough. Therefore we are forced as usual to invoke a slight overshooting to about half a pressure scale height, or less than 1% more in mass depth below the formal lower edge of the convection zone to burn the surface solar lithium. This small overshooting, which is reasonable for the complete braking of the motion, then will reduce slightly the helium and Z elements settling from those calculated with no overshooting.

It appears that the small required overshooting will not affect our comparison between the observed and predicted p-mode frequencies. The lowest l-modes penetrate below the convection zone to almost the solar center, but the highest ones considered do not even exist below this zone. Yet there does not seem to be any significant difference between the low- and high-l comparisons for l less than 200.

Our models require high helium, but also high central temperatures. Thus instead of alleviating the solar neutrino problem we have made it worse, regardless of whether we have diffusive element separation. It appears that to save our models from the criterion of also producing low neutrino fluxes, neutrino oscillations as discussed by Bethe (1986) and Rosen and

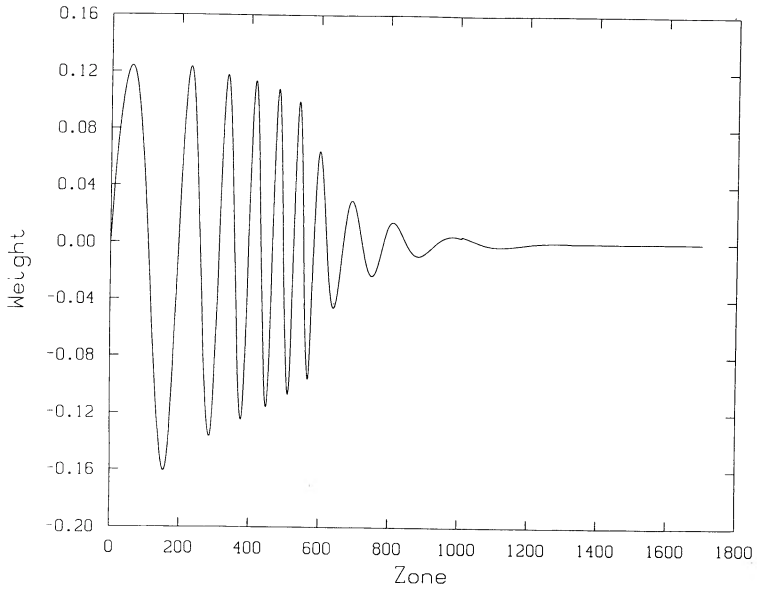

FIG. 20.—The weight for determining the oscillation frequency is plotted vs. mass zone number in the no-diffusion model. Note that the 10 peaks for this g_{10}-mode with degree $l = 2$ sample the entire model deeper than the convection zone, but considerable weight is concentrated close to the center. With accurate g-mode periods, the central solar structure could easily be probed.

Gelb (1986) are needed. A way to reduce this central temperature is to assume the presence of WIMPs that can conduct heat outward. However, the $\delta(n)$ differences suggest that pulsation frequencies do not require WIMPs.

Measurement of the period spacing of the g-modes has been expected to reveal details of the central solar structure, but this work shows that the spacing is not as simple as asymptotic theory (Tassoul 1980) predicts. The variation of the spacing at low mode order and at low l needs to be considered as discussed by Provost and Berthomieu (1986).

Possible improvements of our calculations center on the equation of state for the convection zone and the deep interior. Opacity problems seem not be be so important, but 20% changes could upset the evolving agreement between theoretical predictions and observations.

Classical intrinsically variable stars have their pulsation driving usually within the convection zone, but in those stars convection carries a much smaller fraction of the emergent luminosity, leaving some luminosity for radiation to carry and to be periodically modulated. The temperature derivative of the opacity is the key quantity in determining the mode stability. Slight changes for the behavior given in Figure 6 can change the stability prediction for the p-modes. High-degree solar p-modes have considerable driving exterior to the convection zone, but they also have damping even further out, close to the photosphere, which is caused by steepening the temperature gradient during compression. This radiation-leaking damping is the main mechanism in stabilizing solar p-mode oscillations.

We have investigated the effect of composition on the predictions of instability for the 5 minute p- and f-modes. Use of the Stellingwerf fit for opacities multiplied by 3 gives many unstable modes, but with the original Stellingwerf fit no mode shows any possible instability. The Ross-Aller 1 table, calculated including molecules, gives some p-modes pulsationally unstable and some not. Thus it is not easy to state whether p-modes are pulsationally unstable as a result of the κ- and γ-effects, but the observations suggest that a table like that of King IVa gives the most consistent stability predictions.

It has been believed that f-modes would not have any pulsational driving or damping because they are supposedly motions without any compression. However, as Robe (1965) has shown, there is some variation of density because of the curvature effects, and indeed κ- and γ-effects can occur as we obtain. There is considerable discussion about what to do in the part of the model at the top of the convection zone where the pulsation driving by the κ-effect is important. Unno and Spiegel (1966) developed a theory called the Eddington approximation where the mean intensity of the radiation field differs from the Planck function. Christensen-Dalsgaard and Frandsen (1983) then showed that this approximation gives pulsationally stable p-modes. This theory is valid, however, only when there is no motion of the matter. Mihalas (1984) has discussed this problem and found that with motions, as for pulsations, the Unno and Spiegel analysis should have other terms that also were neglected. It seems that for the present our equilibrium diffusion approximation may be adequate but transport effects must be further investigated.

As a final point, we note that the solar p-mode frequencies are not very sensitive to the helium abundance in the convection zone. The no-diffusion model was recalculated using only the outer 700 zones with $Y = 0.270$ instead of the model value of 0.291. Holding the mixing length fixed here means that at the model center there would not be enough space for all the stellar matter unless compensating composition changes were made somewhere else in the deep interior. For modes with

$l = 60$, which sample just to the convection zone bottom and without excessive dependence on the hydrogen and helium ionization zone equation of state uncertainties, frequencies change by less than 1 μHz. They remain within a few microhertz of the observed frequencies that are reported to be accurate to less than 1 μHz. This partial derivative of the frequency with respect to Y indicates that the inversion problem which determines the solar convection zone helium abundance will not be very easy.

We wish to thank Dean Pesnell, Joërgen Christensen-Dalsgaard, Roger Ulrich, Pierre Demarque, David Guenther, John Bahcall, Walter Huebner, Norman Magee, Al Merts, Bob Roussel-Dupré, Bob Rood, Icko Iben, Dave Schramm, Dave Dearborn, Dimitri and Barbara Mihalas, Steve Becker, Sean Clancy, David Hollowell, Jim MacDonald, Wendee Brunish, Janine Provost, Martin Schwarzschild, Andy White, and Vance Faber for useful discussions.

REFERENCES

Ando, H., and Osaki, Y. 1975, *Pub. Astr. Soc. Japan*, **27**, 581.
Antia, H. M., Chitre, S. M., and Narasimha, D. 1982, *Solar Phys.*, **77**, 303.
Bahcall, J. N., and Holstein, B. R. 1986, *Phys. Rev. C*, **33**, 2121.
Bahcall, J. N., and Ulrich, R. K. 1988, *Rev. Mod. Phys.*, **60**, 297.
Barry, C. T., Rosenwald, R. D., Gu, Y., and Hill, H. A. 1987, *Bull. AAS*, **19**, 1120.
Berthomieu, G., Provost, J., and Schatzman, E. 1984, *Nature*, **308**, 354.
Bethe, H. A. 1986, *Phys. Rev. Letters*, **56**, 1305.
Boesgaard, A. M., and Steigman, G. 1985, *Ann. Rev. Astr. Ap.*, **23**, 319.
Brown, T. M., 1987*a*, in *Stellar Pulsation*, ed. A. N. Cox, W. M., Sparks, and S. G. Starrfield (Berlin: Springer), p. 298.
———. 1987*b*, in *Solar Radiative Output Variation*, ed. P. Foukal (Cambridge: Research and Instrumentation), p. 176.
Burgers, J. M. 1969, in *Flow Equations for Composite Gases* (New York: Academic).
Castor, J. I. 1971, *Ap. J.*, **166**, 109.
Christensen-Dalsgaard, J. 1982, *M.N.R.A.S.*, **199**, 735.
———. 1984, in *Theoretical Problems in Stellar Stability and Oscillations*, ed. A. Noels and M. Gabriel (Liège: Université de Liège), p. 155.
———. 1986, in *Seismology of the Sun and the Distant Stars*, ed. D. O. Gough (Dordrecht: Reidel), p. 23.
Christensen-Dalsgaard, J., Duvall, T. L., Gough, D. O., Harvey, J. W., and Rhodes, E. J. 1985, *Nature*, **315**, 378.
Christensen-Dalsgaard, J., and Frandsen, S. 1983, *Solar Phys.*, **82**, 165.
Christensen-Dalsgaard, J., and Gough, D. O. 1984, in *Solar Seismology from Space*, ed. R. K. Ulrich, J. Harvey, E. J. Rhodes, and J. Toomre (NASA Pub. 84-84), p. 199.
Christensen-Dalsgaard, J., Gough, D. O., and Morgan, J. G. 1979, *Astr. Ap.*, **73**, 121.
Christy, R. F. 1966, *Ap. J.*, **144**, 108.
Clayton, D. D. 1968, *Principles of Stellar Evolution and Nucleosynthesis* (New York: McGraw-Hill).
Cox, A. N. 1965, in *Stars and Stellar Systems*, *Vol.* **8**, *Stellar Structure*, ed. L. H. Aller and D. B. McLaughlin (Chicago: University of Chicago Press), p. 195.
———. 1984, in *Observational Tests of the Stellar Evolution Theory*, ed. A. Maeder and A. Renzini (Dordrecht: Reidel), p. 421.
Cox, A. N., and Kidman, R. B. 1984, in *Theoretical Problems in Stellar Stability and Oscillations*, ed. A. Noels and M. Gabriel (Liège: Université de Liège), p. 259.
Cox, A. N., Kidman, R. B., and Newman, M. J. 1985, in *Solar Neutrinos and Neutrino Astronomy*, ed. M. L. Cherry, W. A. Fowler, and K. Lande (New York: AIP), p. 93.
Cox, A. N., Starrfield, S. G., Kidman, R. B., and Pesnell, W. D. 1987, *Ap. J.*, **317**, 303.
Cox, A. N., and Stewart, J. N. 1965, *Ap. J. Suppl.*, **11**, 22.
Cox, A. N., and Tabor, J. E. 1976, *Ap. J. Suppl.*, **31**, 271.
Cox, J. P. 1980, in *Theory of Stellar Pulsation* (Princeton: Princeton University Press).
Cox, J. P., and Giuli, R. T. 1968 *Principles of Stellar Structure* (New York: Gordon & Breach).
Däppen, W., Gilliland, R. L., and Christensen-Dalsgaard, J. 1986, *Nature*, **321**, 229.
Delache, P., and Scherrer, P. H. 1983, *Nature*, **306**, 651.
Demarque, P. 1960, *Ap. J.*, **132**, 366.
Demarque, P., and Guenther, D. 1986, in *IAU Symposium 123, Advances in Helio- and Asteroseismology*, ed. J. Christensen-Dalsgaard and S. Frandsen (Dordrecht: Reidel), p. 91.
Dilke, F. W. W., and Gough, D. O. 1972, *Nature*, **240**, 262.
Duvall, T. L., Harvey, J. W., Libbrecht, K. G., Popp, B. D., and Pomerantz, M. A. 1988, *Ap. J.*, **324**, 1158.
Eggleton, P. P., Faulker, J., and Flannery, B. P. 1973, *Astr. Ap.*, **23**, 325.
Faulkner, J., and Gilliland, R. L. 1985, *Ap. J.*, **299**, 994.
Faulkner, J., Gough, D. O., and Vahia, M. N. 1986, *Nature*, **321**, 226.
Fontaine, G., and Michaud, G. 1979, in *IAU Colloquium 53, White Dwarfs and Variable Degenerate Stars*, ed. H. M. van Horn and V. Weidema. (Rochester: University of Rochester Press), p. 192.
Fossat, E., Gelly, B., Grec, G., and Pomerantz, M. 1987, *Astr. Ap.*, **177**, L47.
Fowler, W. A., Caughlin, G. R., and Zimmerman, B. A. 1975, *Ann. Rev. Astr. Ap.*, **13**, 113.
Fröhlich, C. 1986, in *Advances in Helio- and Asteroseismology*, ed. J. Christensen-Dalsgaard and S. Frandsen (Dordrecht: Reidel), p. 83.
Gabriel, M. 1984, in *Theoretical Problems in Stellar Stability and Oscillations*, ed. A. Noels and M. Gabriel (Liège: Université de Liège), p. 284.
Gabriel, M., Noels, A., and Scuflaire, R. 1984, *Mem. Soc. Astr. Italiana*, **551**, 169.
Gelly, B., Fossat, E., Grec, G., and Schmider, F.-X. 1988, *Astr. Ap.*, **200**, 207.
Gilliland, R. L., and Däppen, W. 1988, *Ap. J.*, **324**, 1153.
Goldreich, P., and Keeley, D. A. 1977, *Ap. J.*, **211**, 934.
Golub, G. H., and Van Loan, C. F. 1983, *Matrix Computation* (Baltimore: Johns Hopkins University Press).
Graboske, H. C. 1972, *Ap. J.*, **172**, 689.
Guenther, D. B., and Sarajedini, A. 1988, *Ap. J.*, **327**, 993.
Henning, H. M., and Scherrer, P. H. J. 1986, in *Seismology of the Sun and the Distant Stars*, ed. D. O. Gough (Dordrecht: Reidel), p. 55.
Hill, H. A. 1986, in *Neutrino '86: The 12th International Conference on Neutrino Physics and Astrophysics* ed. T. Kitagaki and H. Yuta (Singapore: World Scientific), p. 221.
Hill, H. A., and Gu, Y. M. 1988, *Sci. Sinica*, Ser. A., in press.
Hill, H. A., Tash, J., and Padin, C. 1986, *Ap. J.*, **304**, 560.
Huebner, W. F., Merts, A. L., and Magee, N. H. 1977, Astrophysical Opacity Library, UC-34b.
Iben, I. 1963, *Ap. J.*, **138**, 452.
———. 1965, *Ap. J.*, **141**, 993.
———. 1975, *Ap. J.*, **196**, 546.
Iben, I., Jr., and MacDonald, J. 1985, *Ap. J.*, **296**, 540.
Iben, I., and Mahaffy, J. 1976, *Ap. J. (Letters)*, **209**, L39.
Jefferies, S. M., Pallé, P. L., van der Raay, H. B., Régulo, C., and Roca Cortés, T. 1988, *M.N.R.A.S.*, in press.
Jiménez, A., Pallé, P. L., Perez, J. C., Régulo, C., Roca Corte's, T., Isaak, G. R., McLeod, C. P., and van der Raay, H. B. 1988, in *Advances in Helio- and Asteroseismology*, ed. J. Christensen-Dalsgaard and S. Frandsen (Dordrecht: Reidel), p. 208.
Keeley, D. A. 1977, *Ap. J.*, **211**, 926.
Kidman, R. B., and Cox, A. N. 1984, in *Solar Seismology from Space*, ed. R. K. Ulrich, J. Harvey, E. J. Rhodes, and J. Toomre (NASA Pub. 84-84), p. 335.
———. 1987, in *Stellar Pulsation*, ed. A. N. Cox, W. M. Sparks, and S. G. Starrfield (Berlin: Springer), p. 326.
Korzennik, S. G., and Ulrich, R. K. 1989, *Ap. J.*, **339**, 1144.
Kosovichev, A. G., and Severny, A. B. 1984, in *Theoretical Problems in Stellar Stability and Oscillations*, ed. A. Noels and M. Gabriel (Liège: Université de Liège), p. 278.
Kotov, V. A., Severny, A. B., and Tsap, T. T. 1984, *Mem. Soc. Astr. Italiana*, **55**, 117.
Lebreton, Y., Berthomieu, G., and Provost, J. 1986, in *Advances in Helio- and Asteroseismology*, ed. J. Christensen-Dalsgaard and S. Frandsen (Dordrecht: Reidel), p. 95.
Lebreton, Y., and Maeder, A. 1986, *Astr. Ap.*, **161**, 119.
———. 1987, *Astr. Ap.*, **175**, 99.
Libbrecht, K. G., and Kaufman, J. M. 1988, *Ap. J.*, **324**, 1172.
Mihalas, B. W. 1984, *Ap. J.*, **284**, 299.
Mihalas, D., Däppen, W., and Hummer, D. G. 1988, *Ap. J.*, **331**, 815.
Monchick, L., and Mason, E. A. 1985, *Phys. Fluids*, **28**, 3341.
Muchmore, D. 1984, *Ap. J.*, **278**, 769.
Noels, A., Scuflaire, R., and Gabriel, M. 1984, *Astr. Ap.*, **130**, 389.
Noerdlinger, P. D. 1977, *Astr. Ap.*, **57**, 407.
Paczyński, B. 1969, *Acta Astr.*, **19**, 1.

Pallé, P. L., Pérez, J. C., Régulo, C., Roca Cortés, T., Isaak, G. R., McLeod, C. P., and van der Raay, H. R. 1986, *Astr. Ap.*, **170**, 114.
Pallé, P. L., and Roca Cortés, T. 1986, in *Advances in Helio- and Asteroseismology*, ed. J. Christensen-Dalsgaard and S. Frandsen (Dordrecht: Reidel), p. 79.
Paquette, C., Pelletier, C., Fontaine, G., and Michaud, G. 1986, *Ap. J. Suppl.*, **61**, 177.
Peimbert, M. 1986, *Pub. A.S.P.*, **98**, 1057.
Pesnell, W. D. 1987, *Ap. J.*, **314**, 598.
———. W. D. 1989, *Ap. J. Suppl.*, submitted.
Provost, J. 1984, in *Observational Tests of the Stellar Evolution Theory*, ed. A. Maeder and A. Renzini (Dordrecht: Reidel), p. 47.
Provost, J., and Berthomieu, G. 1986, *Astr. Ap.*, **165**, 218.
Robe, H. 1965, *Bull. Acad. Roy. Belge, de Belgique, Classe des Sci.*, 5th Ser. **51**, 595.
Rosen, S. P., and Gelb, J. M. 1986, *Phys. Rev., D*, **34**, 969.
Rouse, C. A. 1985, *Astr. Ap.*, **149**, 65.
Roussel-Dupré, R. A. 1981, *Ap. J.*, **243**, 329.
———. 1982, *Ap. J.*, **252**, 393.
Saio, H. 1980, *Ap. J.*, **240**, 685.
Schatzman, E. 1985, in *Solar Neutrinos and Neutrino Astronomy*, ed. M. L. Cherry, W. A. Fowler, and K. Lande (New York: AIP), p. 69.
Scuflaire, R., Gabriel, M., and Noels, A. 1984, in *Theoretical Problems in Stellar Stability and Oscillations*, ed. A. Noels and M. Gabriel (Liège: Université de Liège), p. 244.
Severny, A. B., Kotov, V. A., and Tsap, T. T. 1984, *Nature*, **307**, 247.
Shibahashi, H., Noels, A., and Gabriel, M. 1983, *Astr. Ap.*, **123**, 283.
Smeyers, P., and Tassoul, M. 1987, *Ap. J. Suppl.*, **65**, 49.
Stellingwerf, R. F. 1975*a*, *Ap. J.*, **195**, 441.
———. 1975*b*, *Ap. J.*, **199**, 705.
———. 1978, *A.J.*, **83**, 1184.
Stix, M., and Knoelker, M. 1986, in *Physical Processes in Comets, Stars, and Active Galaxies*, ed. W. Hillebrandt, E. Meyer-Hofmeister, and H.-C. Thomas (Berlin: Springer), p. 67.
Tassoul, M. 1980, *Ap. J. Suppl.*, **43**, 469.
Ulrich, R. K., and Rhodes, E. J. 1983, *Ap. J.*, **265**, 551.
Unno, W., Osaki, Y., Ando, H., and Shibahashi, H. 1979, *Nonradial Oscillations of Stars* (Tokyo: University of Tokyo Press).
Unno, W., and Spiegel, E. A. 1966, *Pub. Astr. Soc. Japan*, **18**, 85.
van der Raay, H. B. 1984, in *Theoretical Problems in Stellar Stability* (Liège: Université de Liège), p. 215.
Vardya, M. S. 1964, *Am. J. Phys.*, **32**, 520.
Wambsganss, J. 1988, *Astr. Ap.*, **205**, 125.
Woodard, M. F., and Noyes, R. W. 1985, *Nature*, **318**, 449.

Note added in proof.—While the bulk of the calculations in this paper has been done for the mass zoning given in Figure 3, the g-mode data for Figures 15 and 16 were done with a central ball mass of 1.89×10^{26} in order to increase the frequency precision. The zoning for these later two figures is identical to that for Figure 3 exterior to zone 570.

ARTHUR N. COX: MS B288, Los Alamos National Laboratory, P.O. Box 1663, Los Alamos, NM 87545

JOYCE A. GUZIK: MS B220, Los Alamos National Laboratory, P.O. Box 1663, Los Alamos, NM 87545

RUSSELL B. KIDMAN: MS F611, Los Alamos National Laboratory, P.O. Box 1663, Los Alamos, NM 87545